Computational Studies of Metal−Ligand Bond Enthalpies across the Transition Metal Series

Jamal Uddin, Christine M. Morales, James H. Maynard, and Clark R. Landis*

Department of Chemistry, University of Wisconsin−Madison, 1101 University Avenue, Madison, Wisconsin 53706

Relative to the p-block of the periodic table, data for transition metal−ligand bond dissociation enthalpies are less comprehensive. Recent developments in computational methods make systematic assessment of trends in metal−ligand bond enthalpies across the transition series a relatively rapid and accurate exercise. We report a systematic study of metal−ligand bond enthalpies for saturated transition metal complexes that encompasses the entire d-block of the periodic table and a wide assortment of ligands. The saturated complexes have the form $MH_n−L$ such that closed-shell molecules are formed with the maximum number of two-center, two-electron (2c/2e) bonds under the constraint that the metal electron count does not exceed 12. Bond enthalpies for $MH_n−L$ molecules with higher electron counts (14 and 16 electrons) are assessed for some group 10 and 11 metals. The primary methods are density functional theory (DFT) using the hybrid B3LYP density functional and CCSD(T) ab initio computations. Bond enthalpies are reported as the first bond dissociation enthalpies for neutral and cationic complexes of the type $MH_n−R$ (R = H, CH_3, C_2H_5, $CH(CH_3)_2$, $C(CH_3)_3$, CH_2F, C_2H, C_2H_3, NH_2, OH, F, and BH_2) for all transition elements. Electronic structure analysis of the complexes features natural bond orbital (NBO) analysis of bond polarity.

1. Introduction

Bond enthalpies are valuable quantities to chemists. In part, the value of bond enthalpies derives from the conciseness with which they express the results of thermochemical experiments. For example, understanding of product distributions in free radical additions of HBr to alkenes relies on knowledge of bond enthalpies. Thermodynamics favor the formation of the more stable alkyl radical, leading to the more substituted (Markovnikov) product.[1] More generally, reaction enthalpies can quickly be estimated as the sum of bond enthalpy contributions from bonds that are formed and broken.[2] Such bond additivity estimates are broadly applicable, while more sophisticated group additivity estimates are also available for some classes of organic reactions.[3] This knowledge base aids chemists in developing new reaction processes and determining reaction mechanisms.

Main-group bond enthalpies follow well-defined trends. Underlying these trends is the transferability of 2c/2e bond units. For example, the C−H bonds of methane and cyclohexane have many similar features. More detailed examination of the deviations from perfect transferability has led to some of the most fundamental and enduring concepts of modern chemistry. The concept of electronegativity arose from analysis of trends in homo- and heteronuclear bond enthalpies for simple diatomics.[4] Similarly the concepts of hybridization and resonance provide bases for understanding other trends in bond enthalpies along with other physical properties.

Although "typical" bond enthalpies are well known for main-group atom pairs, the more delocalized bonding typical of organometallic compounds raises new questions. How do metal−ligand bond enthalpies depend on the metal and the "auxiliary" ligands? Do the familiar concepts of bond ionicity, hybridization, and resonance stabilization translate into useful predictors for the thermodynamics of metal−ligand bonding? Homolytic transition metal−ligand bond enthalpies span a wide range, perhaps best illustrated in a critical review by Martinho Simoes and Beauchamp.[5,6] Much of this variation can be attributed to the coordination environment around the metal. Detailed understanding of the factors governing these quantities may allow chemists to "tune" the thermodynamics and kinetics of organometallic reactions.

Organometallic catalysts are widely used for industrially useful organic transformations such as hydrocarbon functionalization and carbon−carbon bond formation.[7] Modification of substrate−catalyst interactions can lead to improvement in the selectivity, catalytic turnover, and rates of these synthetic "toolkit" reactions. For example, Shilov's[8] groundbreaking work in the activation of hydrocarbons was motivated by the assumption that metal−carbon and metal−hydrogen bond enthalpies are reasonably similar. More recently, Marks and co-workers'[9] application of relative M−N and M−C bond enthalpies to the development of catalytic hydroamination reactions using organolanthanide complexes represents a landmark in

(1) (a) Markownikoff, V. V. *Ann. Chem.* **1870**, *153*, 256. (b) McMurray, J. E. *Organic Chemistry*, 6 ed.; Brooks Cole: Monterey, CA, 2003.

(2) Pauling, L. C.; Yost, D. M. *Proc. Natl. Acad. Sci. U.S.A.* **1932**, *18*, 414−416.

(3) (a) Cohen, N.; Benson, S. W. *Chem. Rev.* **1993**, *93*, 2419−2438. (b) Bader, R. F. W.; Bayles, D. *J. Phys. Chem. A* **2000**, *104*, 5579−5589.

(4) Pauling, L. *Nature of the Chemical Bond*, 3rd ed.; Cornell University Press: Ithaca, NY, 1960; Chapter 3.

(5) Connor, J. A. In *Inorganic Chemistry Metal Carbonyl Chemistry*; Boschke, F. L., Dewar, M. J. S., Hafner, K., Heilbronner, E., Ito, S., Lehn, J.-M., Niedenzu, K., Schäfer, K., Wittig, G., Eds.; Springer-Verlag: New York, 1977; Vol. 71.

(6) Martinho Simoes, J. A.; Beauchamp, J. L. *Chem. Rev.* **1990**, *90*, 629−688.

(7) Crabtree, R. H. *J. Organomet. Chem.* **2004**, *689*, 4083−4091.

(8) Shilov, A. E. In *Alkane Activation Processes by Cyclopentadienyl Complexes of Rhodium, Iridium, and Related Species*; Hill; C. L., Ed.; Wiley: New York, 1989; p 372.

(9) Hong, S.; Marks, T. J. *Acc. Chem. Res.* **2004**, *37*, 673−686.

rational catalyst design. Further advancements in catalysis can benefit from a general understanding of homolytic cleavage of metal−carbon, metal−hydrogen, and other metal−ligand bonds.[10]

To investigate trends in metal−ligand bond enthalpies, a comprehensive and consistent data set is required. Ab initio methods, particularly hybrid DFT computations, offer an efficient and fairly accurate means of estimating transition metal−ligand bond enthalpies.[11] Other groups, notably Goddard,[12] Siegbahn,[13] Bauschlichler,[14] and others, have used ab initio calculations to systematically examine metal−hydrogen and metal−carbon bond enthalpies in the absence of any spectator ligands. Harvey,[15] Ziegler,[16,17] Clot, and others[18] have used pure and hybrid DFT methods to obtain metal−ligand bond enthalpies for collections of coordinatively saturated compounds.

We present a new, systematic collection of metal−ligand homolytic bond enthalpies obtained by DFT computations. Model compounds, spanning the entire transition series, have been chosen in such a way as to facilitate comparison between metal−ligand bonds and the well-known, localized, 2c/2e bonds of main-group compounds. Background information is presented in Section 2; this includes concepts emerging from experimental studies and computations in the literature along with the Lewis-like formulation of transition metal models. Section 3 describes the computational method. Section 4 presents calculated homolytic M−L bond enthalpies with L = H, CH_3, C_2H_5, CH(CH_3)$_2$, C(CH_3)$_3$, C_2H, C_2H_3, CH_2F, BH_2, NH_2, OH, and F. The discussion in Section 5 examines the applicability of familiar localized bond concepts to the estimation of such metal−ligand bond enthalpies. Throughout this presentation, electronic effects are discussed in terms of systematic trends in bond enthalpies rather than extensive analysis of electron density distributions. Section 6 concludes this work and summarizes prospects for further study.

2. Background

A. "Valency-Saturated" MH$_n$−X Models for Exploring Bond Enthalpies. A simple localized bond model for simple transition metal hydrides and alkyls, featuring Lewis-like structures and sd^n hybridization of metal orbitals, provides a zeroth-order description of electron density distributions.[19] This model, which is supported by extensive analyses of high-quality ab initio electronic structure computations, hypothesizes that six valence s and d orbitals are used by the metal for bonding. This hypothesis dictates a filled valence electron count of 12 electrons (12e) for a metal making electron pair bonds, much as an octet of electrons marks filling of the valence electron

count in most p-block elements. In analogy with the s- and p-blocks, d-block MH$_n$ complexes with fewer than 12e counts are hypovalent, whereas counts in excess of 12e are hypervalent. The importance of these classifications is that electron counts greater than 12e signal a significant change in bonding from well-localized 2c/2e units to more delocalized three-center, four-electron (3c/4e) bonding arrangements. For electron counts of 12e and less, simple hybridization of s and d orbitals provides a remarkably robust method for predicting the complex, multiple minima observed for simple metal hydrides such as WH_6.[19d] Some examples of Lewis-like structures and M−H bond hybridizations of MH$_n$ complexes having electron counts of 12e or less are shown below. These structures illustrate the maximum number of covalent bonds formed under the 12-electron rule for each of the third-row transition metals from La to Pt.
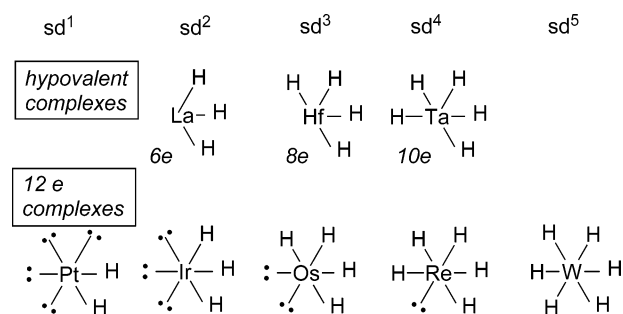
We refer to complexes of the type shown above as valency-saturated complexes in the sense that, within the limits of using only s and d orbitals to make only 2c/2e bonds, the metal uses available valence electrons to make the maximum number of bonds. This terminology distinguishes between "valency-saturated" and "coordinatively saturated" in that "valency-saturated" refers to maximal use of the neutral metal atom's electrons in making localized 2c/2e bonds, whereas coordinatively saturated commonly refers to the metal achieving the maximal number of coordinated ligands, often achieving an 18-electron count.

Because the focus of the present model is on the electron count, examination of charge effects centers on the comparison between *isoelectronic* charged and neutral species. Charged species are chosen for which the isoelectronic neutral compound is valency-saturated. It should be noted that if H$_n$M$^+$−X and H$_n$M′−X are isoelectronic, then M′ is the metal to the left of M in the periodic table. For example HfH$_4$ and TaH$_4^+$ are based on different metals but possess the same electron and ligand count. In addition to the overall molecular charge, metal-specific properties such as the effective nuclear charge may have an effect on metal−ligand bond enthalpies.

In the context of investigation of metal−ligand bond enthalpies, the valency-saturated complexes of the form H$_n$M−X are attractive because (1) they represent a consistent set of base electronic structures for which valency is saturated, (2) exchange and promotion effects are minimized across the d-block due to

(10) Marks, T. J. In *Bonding Energetics in Organometallic Compounds*; Marks, T. J., Ed.; American Chemical Society: Washington, D.C., 1990; Vol. 428.

(11) Ziegler, T. In *Computational Thermochemistry: Prediction and Estimation of Molecular Thermodynamics*; Irikura, K. K., Frurip, D. J., Eds.; American Chemical Society: Washington, DC, 1998; Vol. 677, p 470.

(12) (a) Schilling, J. B.; Goddard, W. A., III; Beauchamp, J. L. *J. Am. Chem. Soc.* **1986**, *108*, 582−584. (b) Schilling, J. B.; Goddard, W. A., III; Beauchamp, J. L. *J. Phys. Chem.* **1987**, *91*, 5616−5623. (c) Schilling, J. B.; Goddard, W. A.; Beauchamp, J. L. *J. Am. Chem. Soc.* **1987**, *109*, 5565−5573. (d) Schilling, J. B.; Goddard, W. A., III; Beauchamp, J. L. *J. Am. Chem. Soc.* **1987**, *109*, 5573−5580.

(13) Siegbahn, P. E. M. *J. Phys. Chem.* **1995**, *99*, 12723−12729.

(14) Bauschlicher, C. W. J.; Langhoff, S. R.; Partridge, H.; Barnes, L. A. *J. Chem. Phys.* **1989**, *91*, 2399−2411.

(15) Harvey, J. N. *Organometallics* **2001**, *20*, 4887−4895.

(16) (a) Ziegler, T.; Tschinke, V.; Becke, A. *J. Am. Chem. Soc.* **1987**, *109*, 1351−1358. (b) Ziegler, T.; Cheng, W.; Baerends, E. J.; Ravenek, W. *Inorg. Chem.* **1988**, *27*, 7.

(17) Folga, E.; Ziegler, T. *J. Am. Chem. Soc.* **1993**, *115*, 5169−5176.

(18) Clot, E.; Mégret, C.; Eisenstein, O.; Perutz, R. N. *J. Am. Chem. Soc.* **2006**, *128*, 8350−8357.

(19) (a) Root, D. M.; Landis, C. R.; Cleveland, T. *J. Am. Chem. Soc.* **1993**, *115*, 4201−4209. (b) Landis, C. R.; Cleveland, T.; Firman, T. K. *J. Am. Chem. Soc.* **1995**, *117*, 7. (c) Cleveland, T.; Landis, C. R. *J. Am. Chem. Soc.* **1996**, *118*, 6020−6030. (d) Landis, C. R.; Cleveland, T.; Firman;, T. K.; Seppelt, K. *Science* **1996**, *272*, 179f−183. (e) Landis, C. R.; Firman, T. K.; Root, D. M.; Cleveland, T. *J. Am. Chem. Soc.* **1998**, *120*, 1842−1854. (f) Landis, C. R.; Cleveland, T.; Firman, T. K. *J. Am. Chem. Soc.* **1998**, *120*, 2641−2649. (g) Firman, T. K.; Landis, C. R. *J. Am. Chem. Soc.* **1998**, *120*, 12650−12656. (h) Firman, T. K.; Landis, C. R.; *J. Am. Chem. Soc.* **2001**, *123*, 11728−11742. (i) Weinhold, F. A.; Landis, C. R. *Valency and Bonding: A Natural Bond Orbital Donor−Acceptor Perspective*; Cambridge University Press, 2005.

the closed-shell nature of the complexes and the consistent underlying s^1d^n atomic configuration (where n = group number − 1) of the metal, (3) steric influences of the ligands are minimized due to the small size of the H ligands, (4) charge effects are minimized, as M−H bonds are commonly apolar except for the earlier transition metals, (5) the structures of MH_n complexes have been extensively investigated and are well understood, and (6) computations on such complexes are reasonably fast, thus enabling extensive evaluations of bond enthalpy trends. We recognize that many of these models have not been observed experimentally and, hence, preclude comparison of our computations with empirical values. We also recognize that the computation of transition metal bond enthalpies at the level of "chemical accuracy" currently is an unsolved problem. However, the methods used herein are quite robust and informative for the semiquantitative purposes of this work.

B. How Do Metal Orbitals Influence Bond Enthalpies? In the Lewis-like model of d-block bonding described above, metal d orbitals and the d electron count play a key role. Just as the electron count on the metal affects molecular structure, it may also contribute to the energy of bonding orbitals. Ideally, such behavior should lead to predictable trends in homolytic metal−ligand bond enthalpies as the metal is varied across a row of the periodic table.

Some evidence exists for the concept of an "intrinsic" bond enthalpy that is constant across a given row of the transition series. In particular, Armentrout and co-workers[20−23] have collected and analyzed a large body of bond enthalpies for the simple molecules M^+−H, M^+−CH_3, M−H, and M−CH_3. For highly unsaturated (in both the valence and coordinated senses) organometallic complexes of these types, bond dissociation yields the charged or neutral metal atom, with relaxation to the ground electronic configuration and/or recovery of exchange energy associated with a higher spin multiplicity. Such exchange and promotion contributions (designated E_p) to bond dissociation energy have been explored theoretically by Goddard and others.[24,25] For metals in a given row, fluctuations in the measured bond enthalpies correlate surprisingly well with E_p. Upon extrapolating the best-fit line to $E_p = 0$, a value thought of as the "intrinsic" bond enthalpy is obtained. Because no change in exchange or promotion energy is expected for homolytic cleavage in closed-shell compounds of the form L_nM−R, such bond enthalpies would be expected to match the intrinsic bond enthalpy for all metals in a given row. Despite the appealing simplicity of the above model, it does not seem to account for the wide range of bond enthalpies that have been measured for coordinatively saturated organometallic compounds of the form L_nM−R. For example, Stevens and Beauchamp[26] found that L_nM^+−H bond enthalpies, measured in the gas phase for first- and second-row metals M, vary widely between 53 and 85 kcal/mol with an average of 68 kcal/mol.

Bond polarity provides a basis for periodic trends in main-group bond enthalpies to be understood. Can this framework be extended to homolytic metal−ligand bond enthalpies in organometallic species? When relative metal−carbon (M−C) bond enthalpies in organometallic complexes of the form L_nM−R are compared to hydrogen−carbon (H−C) bond enthalpies in the corresponding hydrocarbons H−R, (M−C) bond enthalpies generally increase with the corresponding hydrocarbon H−C bond enthalpies. Bercaw and others[27] first performed a number of solution-phase measurements, obtaining M−C/H−C correlations that approach linearity and a 1:1 ratio for a series of substituents. Other investigators, such as Bergman and co-workers,[28,29] have obtained M−C/H−C correlations (and M−X/H−X correlations, for heteroatoms X = N, O, and F) that yield a ratio near 2:1, suggesting that some metals are potentially useful for activation of strong C−H bonds. Related theoretical studies by Harvey,[15] Ziegler,[11] and others suggest that bond polarity may contribute to these trends (vide infra).

For organometallic compounds with full ligand sets, the dependence of bond enthalpies on auxiliary ligands must also be considered. Unquestionably, bulky ligands exert a powerful steric influence on molecular structure. "Bond strength" terms may be derived from bond enthalpies by correcting for geometric reorganization energy regained upon bond cleavage.[5] Electronic effects of auxiliary ligands on metal−ligand bond enthalpies also are observed. For example, ligand effects on the Lewis acidity of organometallics have been rationalized using Pearson's[30−32] empirical hard soft acid base (HSAB) principle. A particularly interesting concept is the *trans*-influence, commonly associated with square-planar d^8 metal complexes such as $[PtH_2Cl_2]^{2-}$ but also observed for octahedral complexes.[33] Notably, Halpern and co-workers[34] have found that axial ligands exert a strong influence on the Co−R bond enthalpy in model compounds for coenzyme B_{12}. Within a covalent bonding model, concepts such as hybridization and resonance stabilization might help chemists to understand how "spectator" ligands perturb metal−ligand bond enthalpies.

C. Evidence for Periodic Trends in Metal−Ligand Bond Enthalpies.

i. Homolytic M−H Bond Enthalpies. Studies of "intrinsic" bond enthalpies suggest the useful periodic trend whereby stronger M−H bonds are formed by second- and third-row metals. First-row M^+−H bond enthalpies, extrapolated to zero E_p, point to an intrinsic bond enthalpy of 56 kcal/mol, and a similar value of 58 kcal/mol has been found for neutral M−H.[20] For second-row metals, the M^+−H intrinsic bond enthalpy is somewhat higher, 62 kcal/mol.[23] The few M−H and M^+−H bond enthalpies available for third-row metals appear to be higher than for second-row metals.[37] This periodic trend seems generally to apply to bond enthalpies in coordinatively saturated

(20) Armentrout, P. B.; Kickel, B. L. In *Organometallic Ion Chemistry*; Freiser, B. S., Ed.; Kluwer Academic Publishers: Boston, 1996.

(21) Elkind, J. L.; Armentrout, P. B. *Inorg. Chem.* **1986**, *25*, 1078−1080.

(22) Armentrout, P. B. In *Bonding Energetics in Organometallic Compounds*; Marks, T. J., Ed.; American Chemical Society: Washington, DC, 1990; Vol. 428.

(23) Armentrout, P. B.; Sunderlin, L. S. In *Transition Metal Hydrides*; Dedieu, A., Ed.; VCH: New York, 1992.

(24) (a) Carter, E. A.; Goddard, W. A., III. *J. Phys. Chem.* **1988**, *92*, 2, 5679−5683. (b) Ohanessian, G.; Goddard, W. A., III. *Acc. Chem. Res.* **1990**, *23*, 386-392.

(25) Ohanessian, G.; Brusich, M. J.; Goddard, W. A. I. *J. Am. Chem. Soc.* **1990**, *112*, 7179−7189.

(26) Stevens, A. E.; Beauchamp, J. L. *J. Am. Chem. Soc.* **1981**, *103*, 190−192.

(27) (a) Bryndza, H. E.; Fong, L. K.; Paciello, R. A.; Tam, W.; Bercaw, J. E. *J. Am. Chem. Soc.* **1987**, *109*, 1444−1456. (b) Bryndza, H. E.; Domaille, P. J.; Tam, W.; Fong, L. K.; Paciello, R. A.; E. Bercaw, J. *Polyhedron* **1988**, *7*, 1441−1452.

(28) Stoutland, P. O.; Bergman, R. G.; Nolan, S. P.; Hoff, C. D. *Polyhedron* **1988**, *7*, 1429−1440.

(29) Holland, P. L.; Andersen, R. A.; Bergman, R. G.; Huang, J. K.; Nolan, S. P. *J. Am. Chem. Soc.* **1997**, *119*, 12800−12814.

(30) Pearson, R. G. *J. Chem. Educ.* **1968**, *45*, 581−587.

(31) Pearson, R. G. *Inorg. Chem.* **1973**, *12*, 712−713.

(32) Pearson, R. G. *Chem. Rev.* **1985**, *85*, 41−49.

(33) Appleton, T. G.; Clark, H. C.; Manzer, L. E. *Coord. Chem. Rev.* **1973**, *10*, 335−422.

(34) Halpern, J. *Acc. Chem. Res.* **1982**, *15*, 238−244.

(35) Tilset, M.; Parker, V. D. *J. Am. Chem. Soc.* **1989**, *111*, 6711−6717.

(36) Skagestad, V.; Tilset, M. *J. Am. Chem. Soc.* **1993**, *115*, 5077−5083.

(37) Armentrout, P. B. *Int. J. Mass Spectrom.* **2003**, *227*, 289−302.

species of the form $L_nM−H$. For example, Tilset and Parker[35] found a definite increase down a period from first- to second- to third-row metals.

The effect of overall molecular charge on $L_nM^+−H$ versus $L_nM−H$ bond enthalpies also has been investigated. The similarity of first-row "intrinsic" $M^+−H$ and $M−H$ bond enthalpies suggests that metal−hydrogen bond enthalpies in cationic species are comparable to (or slightly weaker than) those in neutral diatomics. For coordinatively saturated complexes, one-electron oxidation is generally found to reduce the bond enthalpy. For example, in a study using bulky $TpM(CO)_3H$ complexes (M = Cr, Mo, W), Skagestad and Tilset[36] found that one-electron oxidation decreased the homolytic $TpM(CO)_3−H$ bond enthalpy predictably by 6−8 kcal/mol. On the basis of the comparison between $(CO)_5Fe^+−H$ and $(CO)_5Ni^+−H$ and the isoelectronic neutrals $(CO)_5Mn−H$ and $(CO)_5Co−H$, Stevens and Beauchamp[26] predicted that $L_nM^+−H$ bond enthalpies may be 10−15 kcal/mol stronger than $L_nM−H$ bond enthalpies for the isoelectronic, neutral compounds. However, no obvious trend was found by Martinho Simoes and Beauchamp[6] based on metal−hydrogen bond enthalpies in the isoelectronic species $(CO)_4Fe^−−H$, $(CO)_4Co−H$, and $(CO)_4Ni^+−H$.

ii. Homolytic M−CH₃ Bond Enthalpies. The periodic trend in metal−methyl bond enthalpies on descending a group is similar to that found for metal−hydrogen bond enthalpies. Intrinsic $M−CH_3$ and $M^+−CH_3$ bond enthalpies for second- and third-row transition metals tend to be stronger than the corresponding quantities for first-row metals.[37] This general periodic trend also is borne out for coordinatively saturated species.[6]

One-electron oxidation seems to affect metal−methyl bond enthalpies in a different manner for metal−methyl species of the form $M−CH_3$ and $M^+−CH_3$ than for coordinatively saturated species. For the simplest first-row metal−methyl complexes $M−CH_3$ and $M^+−CH_3$, intrinsic bond enthalpies are 49 and 58 kcal/mol, respectively.[22,38] In contrast, one-electron oxidation weakens metal−methyl bonds for coordinatively saturated compounds of the form $L_nM−CH_3$.[6] Theoretical studies suggest that the polarizability of the $−CH_3$ group confers added stability to $M^+−CH_3$ bonds.[12d,14]

Charge and auxiliary ligands as well as the metal center can influence the relative strengths of metal−methyl and corresponding metal−hydrogen bond enthalpies. Metal−methyl bonds in species of the form $M^+−CH_3$ are stronger than the corresponding $M^+−H$ bonds.[39] However, metal−methyl bond enthalpies in neutral compounds of the form $M−CH_3$ or $L_nM−CH_3$ are generally weaker than the analogous $L_nM−H$ and $M−H$ bond enthalpies.[6] For example, the metal−methyl bond in $(CO)_5Mn−CH_3$ was measured to be 14 kcal/mol weaker than the metal−hydrogen bond in $(CO)_5Mn−H$.[40] This difference between $L_nM−CH_3$ and $L_nM−H$ bond enthalpies is smaller for early transition metals than for late metals.[41]

iii. Homolytic Metal−Hydrocarbyl and Metal−Hetero-atom Bond Enthalpies. Relative bond enthalpies have been reported for various organometallic compounds of the form $L_nM−R$, along with comparisons to the corresponding H−R

bond enthalpies. Although such correlations are not perfectly linear, best-fit lines have been reported and their slopes are referred to herein as $\mathscr{R}^{MC/HC}$. No unifying theory has been formulated that explains the variation of $\mathscr{R}^{MC/HC}$ in such correlations, but it is interesting to note that $\mathscr{R}^{MC/HC}$ values are generally smaller for complexes of early transition metals than for late metals. In a study of $Cp^*_2Zr−R$ and $Cp^*_2Hf−R$ bond enthalpies ($−R = −CH_3$, $−CH_2CH_2CH_2CH_3$, and $−Ph$), Marks and co-workers[41] obtained $\mathscr{R}^{MC/HC} = 0.64$ and rationalized the trend in terms of bond polarity. Although those authors predicted $\mathscr{R}^{MC/HC} < 1$ for electropositive early metals, other groups have reported correlations with $\mathscr{R}^{MC/HC} \geq 1$. For example, a correlation with a slope $\mathscr{R}^{MC/HC} \approx 1$ was found by Wolczanski and co-workers[42,43] in compounds of the form $(^tBu_3SiN)_2(^tBu_3SiNH)$-$Ta−R$, $(^tBu_3SiNH)_3Zr−R$, and $(^tBu_3SiO)_2(^tBu_3SiNH)Ti−R$, for a variety of sp-, sp²-, and sp³-hybridized hydrocarbyl substituents $−R$. In a study of $Cp^*(\eta^5,\eta^1\text{-}C_5Me_4CH_2CH_2CH_2)Sc−R$ bond enthalpies with sp²- and sp³-hybridized hydrocarbyl fragments, Bercaw and co-workers[44] found an even steeper correlation with $\mathscr{R}^{MC/HC} = 1.25$. In several studies of group 9 metals, linear best-fit correlations have been reported with $\mathscr{R}^{MC/HC} \geq 1$. Notably, Bergman and co-workers[45] reported a ratio $\mathscr{R}^{MC/HC} = 2$ in the correlation between $(Cp^*)(PMe_3)Ir−R$ and H−R bond enthalpies, for sp²- and sp³-hybridized hydrocarbyl fragments. A more modest $\mathscr{R}^{MC/HC} = 1.22$ was reported by Jones and co-workers[46] in a study of $Tp'(CNCH_2CMe_3)Rh−R$ bond enthalpies, with sp²- and sp³-hybridized hydrocarbyls.

Analogously, $L_nM−X$ bond enthalpies have been compared to the corresponding H−X bond enthalpies for halide, hydroxyl, and amino substituents −X, yielding linear best-fit correlations with slopes $\mathscr{R}^{MX/HX}$ between 0 and 2. For $Cp^*_2Zr−X$ and Cp^*_2-$Hf−X$ bond enthalpies, Marks and co-workers[41] determined a ratio $\mathscr{R}^{MX/HX} = 0.77$ for X = OR and NH_2; $\mathscr{R}^{MX/HX} = 1.07$ was found for the halides. Bergman and co-workers[47] found a ratio $\mathscr{R}^{MX/HX} = 1.9$ for $Cp^*(PEt_3)Ni−X$ bond enthalpies, with X = CH_3, $N(CH_3)_2$, OCH_3, F, and CF_3. However, Bercaw and co-workers[48] found $\mathscr{R}^{MX/HX} \approx 1$ for $(dppe)(Me)Pt−X$ or (Cp^*)-$(PMe_3)_2Ru−X$ bond enthalpies, with X = H, $CH_2C(O)CH_3$, CCPh, CN, OH, OCH_3, NHMe, NHPh, NPh_2, and SH. Similarly, Mayer and co-workers[49] reported $\mathscr{R}^{MX/HX} \approx 1$ for $(MeCCMe)_2$-$(O)Re−X$, with X = NRR′ and OR.

Several ab initio studies have provided theoretical transition metal−carbon bond enthalpies for systematic collections of hydrocarbyl substituents, metal centers, and ligand sets. Recent work by Clot and co-workers, using the B3PW91 functional, has found $\mathscr{R}^{MC/HC}(calc) \approx \mathscr{R}^{MC/HC}(expt) > 1$ for compounds of the form $Tp'(CNCH_2CMe_3)Rh−R$ and $(silox)_2(^tBu_3SiNH)$-$Ti−R$.[18] Siegbahn's[50] correlated ab initio study of second-row metal−hydrocarbyl bond enthalpies highlighted metal-dependent

(38) (a) Armentrout, P. B.; Halle, L. F.; Beauchamp, J. L. *J. Am. Chem. Soc.* **1981**, *103*, 6501−6502. (b) Armentrout, P. B.; Georgiadis, R. *Polyhedron* **1988**, *7*, 1573−1581.

(39) Mandich, M. L.; Halle, L. F.; Beauchamp, J. L. *J. Am. Chem. Soc.* **1984**, *106*, 4403−4411.

(40) Connor, J. A.; Zafarani-Moattar, M. T.; Bickerton, J.; El Saied, N. I.; Suradi, S.; Carson, R.; Al Takhin, G.; Skinner, H. A. *Organometallics* **1982**, *1*, 1166−1174.

(41) Schock, L. E.; Marks, T. J. *J. Am. Chem. Soc.* **1988**, *110*, 7701−7715.

(42) (a) Schaller, C. P.; Wolczanski, P. T. *Inorg. Chem.* **1993**, *32*, 131−144. (b) Schaller, C. P.; Cummins, C. C.; Wolczanski, P. T. *J. Am. Chem. Soc.* **1996**, *118*, 591−611.

(43) Bennett, J. L.; Wolczanski, P. T. *J. Am. Chem. Soc.* **1997**, *119*, 10696−10719.

(44) Bulls, A. R.; Bercaw, J. E.; Manriquez, J. M.; Thompson, M. E. *Polyhedron* **1988**, *7*, 1409−1428.

(45) Stoutland, P. O.; Bergman, R. G.; Nolan, S. P.; Hoff, C. D. *Polyhedron* **1988**, *7*, 1429−1440.

(46) Wick, D. D.; Jones, W. D. *Organometallics* **1999**, *18*, 495−505.

(47) Holland, P. L.; Andersen, R. A.; Bergman, R. G.; Huang, J. K.; Nolan, S. P. *J. Am. Chem. Soc.* **1997**, *119*, 12800−12814.

(48) (a) Bryndza, H. E.; Fong, L. K.; Paciello, R. A.; Tam, W.; Bercaw, J. E. *J. Am. Chem. Soc.* **1987**, *109*, 1444−1456. (b) Bryndza, H. E.; Domaille, P. J.; Tam, W.; Fong, L. K.; Paciello, R. A.; E. Bercaw, J. *Polyhedron* **1988**, *7*, 1441−1452.

(49) Erikson, T. K. G.; Bryan, J. C.; Mayer, J. M. *Organometallics* **1988**, *7*, 1930−1938.

(50) Siegbahn, P. E. M. *J. Phys. Chem.* **1995**, *99*, 12723−12729.

electronic effects. Relative M^+-R bond enthalpies increased more quickly than the corresponding $H-R$ bond enthalpies, leading to ratios $\mathscr{R}^{MC/HC} > 1$ that are larger for early metals than for late metals. A density functional theory study by Harvey[51] explored steric effects in coordinatively saturated metal compounds and used Natural Population Analysis (vide infra) to obtain metal–alkyl bond enthalpies and partial charges. Enthalpic trends for $Cp_2Zr(H)-R$ were found consistent with a simple electrostatic model. For a series of Fe^{II} complexes with larger ligand sets, deviations from the electrostatic model were attributed to steric effects. The above analyses agree that as the hydrocarbyl substituent is varied, metal–carbon bond enthalpies increase with bond polarity.

Although ab initio studies indicate some relationship between transition metal–ligand bond enthalpies and bond polarity, empirical relationships[2] between main-group bond enthalpies and electronegativity differences have yet to be extended to coordinatively saturated organometallics. Limited sets of transition metal–ligand bond enthalpy data have been analyzed with respect to models that were originally derived for main-group bond enthalpies. For simple diatomics of the form $M-H$, Pearson[32] compared absolute $M-H$ bond enthalpies to Mulliken electronegativities, while Squires[52] used electron affinities. Various research groups have fit their own L_nM-H and L_nM-R bond enthalpies to different formulas due to Pauling,[41] Matcha,[53] and Drago;[54] however, no one model has been used to fit all data simultaneously. The lack of a simple empirical formula may indicate a more complicated trend than is found among main-group elements.

3. Computational Methods

Density functional theory using the B3LYP hybrid functional was employed under a spin-restricted or restricted open-shell formalism for all calculations.[55] Gaussian-98[56] was used for CCSD-(T) and MP2 calculations, while Jaguar 4.2[57] was used for all other calculations. The nonstandard Jaguar SCF options iacc=1 and nops=1 was used to request fully analytic SCF calculations using ultrafine grid and cutoffs. All calculations were carried out using the triple-ζ LACV3P++** basis set for the valence and outermost core shell electrons on transition metals and the LANL effective core potential in place of the inner-core electrons.[58] This basis employs 6-311++G** basis functions for main-group elements.[59] Ground-state energies for metal radical fragments are taken as the minimum B3LYP energy obtained for low-lying electronic configurations. Total energies are reported without zero-point corrections. The resulting bond dissociation energies are in fact D_e values,

Figure 1. H_nM-H bond enthalpies (kcal/mol) calculated at B3LYP and CCSD(T) levels of theory with the triple-ζ LACV3P++** basis set, for valency-saturated hydride compounds of selected first-, second-, and third-row transition metals M, as indicated on the abscissa. Filled circles represent B3LYP values, and open circles represent CCSD(T) values.

therefore differing from 0 K bond dissociation enthalpies, D_0; however, the corrections are expected to be small. We have used the term "bond enthalpy" to refer both to the calculated D_e values and to D_0 or D_{298} values obtained from the literature.

Global minima on the potential energy surface have previously been located by us and by other workers for many of the valency-saturated transition metal hydrides.[19b,e,i,60] Conformational searching was repeated for all metals, and only classical hydride structures were considered.[61] Regardless of their relative stability, structures involving H_2 σ-adducts, $R-H$ σ-adducts, agostic $(\eta^2\text{-}R-H)-MH_n$ and bridging $B-H-MH_n$ moieties were eliminated for simplicity.[62] Where classical local minima could not be located, constrained optimizations were used to locate a pseudoclassical structure. The limitation of our study to classical hydrides allows us to capture the energetic effects associated with homolytic metal–ligand bonding, and we estimate only a 5–10 kcal/mol difference between conformers. All structures were confirmed to be true minima by the absence of imaginary frequencies in an approximate normal-mode analysis, using the updated Hessian upon full optimization. Several benchmark studies are available in the literature to support the performance of the B3LYP functional for the computation of homolytic transition metal–ligand bond enthalpies.[63] Additionally, MP2 geometry optimizations and CCSD(T) single-point energies were computed from the B3LYP-optimized geometries for selected species, for comparison to B3LYP geometries and energies. The

(51) Harvey, J. N. *Organometallics* **2001**, *20*, 4887–4895.

(52) Squires, R. R. *J. Am. Chem. Soc.* **1985**, *107*, 4385–4390.

(53) Labinger, J. A.; Bercaw, J. E. *Organometallics* **1988**, *7*, 926–928.

(54) Holland, P. L.; Andersen, R. A.; Bergman, R. G. *Comments Inorg. Chem.* **1999**, *21*, 115–129.

(55) (a) Becke, A. D. *J. Chem. Phys.* **1993**, *98*, 5648–5652. (b) Becke, A. D. *J. Chem. Phys.* **1993**, *98*, 1372–1377. (c) Becke, A. D. *Phys. Rev. A* **1998**, *38*, 3098–3100.

(56) Frisch, M. J.; Trucks, G. W.; Schlegel, H. B.; Scuseria, G. E.; Robb, M. A.; Cheeseman, J. R.; Zakrzewski, V. G.; Montgomery, J. A., Jr.; Stratmann, R. E.; Burant, J. C.; Dapprich, S.; Millam, J. M.; Daniels, A. D.; Kudin, K. N.; Strain, M. C.; Farkas, O.; Tomasi, J.; Barone, V.; Cossi, M.; Cammi, R.; Mennucci, B.; Pomelli, C.; Adamo, C.; Clifford, S.; Ochterski, J.; Petersson, G. A.; Ayala, P. Y.; Cui, Q.; Morokuma, K.; Malick, D. K.; Rabuck, A. D.; Raghavachari, K.; Foresman, J. B.; Cioslowski, J.; Ortiz, J. V.; Baboul, A. G.; Stefanov, B. B.; Liu, G.; Liashenko, A.; Piskorz, P.; Komaromi, I.; Gomperts, R.; Martin, R. L.; Fox, D. J.; Keith, T.; Al-Laham, M. A.; Peng, C. Y.; Nanayakkara, A.; Gonzalez, C.; Challacombe, M.; Gill, P. M. W.; Johnson, B. G.; Chen, W.; Wong, M. W.; Andres, J. L.; Head-Gordon, M.; Replogle, E. S.; and Pople, J. A. *Gaussian 98* (Revision A.7); Gaussian, Inc.: Pittsburgh, PA, 1998.

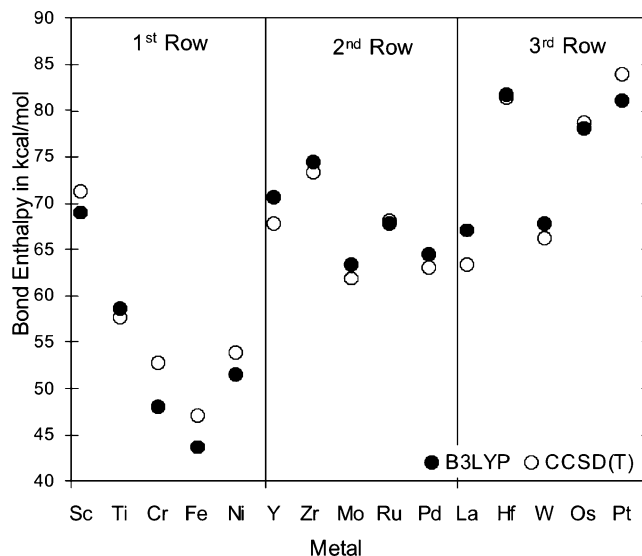(57) *Jaguar 4.2*; Schrödinger Inc.: Portland, OR, 1991–2000.

(58) (a) The LACV3P basis set is a triple-ζ contraction of the LACVP (LANL2DZ) basis set developed and tested at Schrödinger, Inc. See the Supporting Information for details. (b) Dunning, T. H., Jr.; Hay, P. J. In *Modern Theoretical Chemistry*; Schaefer, H. F., Ed.; Plenum: New York, 1977. (c) Hay, P. J.; Wadt, W. R. *J. Chem. Phys.* **1985**, *82*, 270–283. (d) Wadt, W. R. and Hay, P. J. *J. Chem. Phys.* **1985**, *82*, 284–298. (e) Hay, P. J.; Wadt, W. R. *J. Chem. Phys.* **1985**, *82*, 299–310.

(59) (a) Krishnan, R.; Binkley, J. S.; Seeger, R.; Pople, J. A. *J. Chem. Phys.* **1980**, *72*, 650–654. (b) Clark, T.; Chandrasekhar, J.; Spitznagel, G. W.; Schleyer, P. v. R. *J. Comput. Chem.* **1983**, *4*, 294–301. (c) Frisch, M. J.; Pople, J. A.; Binkley, J. S. *J. Chem. Phys.* **1984**, *80*, 3265–3269.

(60) Kaupp, M. *Angew. Chem., Int. Ed.* **2001**, *40*, 3535–3565.

(61) Lin, Z.; Hall, M. B. *Coord. Chem. Rev.* **1994**, *135/136*, 845–879.

(62) H–H distances of less than 1.5 Å were considered indicative of molecular H_2 adduct formation.

(63) (a) Barone, V.; Adamo, C. *Int. J. Quantum Chem.* **1997**, *61*, 443–451. (b) Koch, W.; Holthausen, M. C. *A Chemist's Guide to Density Functional Theory*; Wiley-VCH: New York, 2001; Chapter 9.3.

same triple-ζ LACV3P++** basis set[59] was used for MP2, CCSD-(T), and B3LYP calculations. For selected neutral, valency-saturated transition metal polyhydrides, first bond dissociation enthalpies at the B3LYP level of theory were compared with those obtained using CCSD(T) single-point energies at the B3LYP-optimized geometries. As shown in Figure 1, bond dissociation enthalpies were remarkably similar at both levels of theory, generally giving values within a few kcal/mol.

i. Natural Bond Orbital Analysis. Natural bond orbital (NBO) analysis, a collection of orbital localization methods by Weinhold and co-workers, involves the formation of natural atomic orbital (NAO), natural hybrid orbital (NHO), and natural bond orbital (NBO) basis sets.[64] NBO methods are based on the first-order reduced density matrix,[65] Γ, in an atom-centered atomic orbital (AO) basis. NAO, NHO, and NBO basis sets each consist of a minimal basis set of nearly singly occupied spin–orbitals and a virtual basis set of nearly unoccupied spin–orbitals. Within each basis set, the orbitals are all orthogonal, guaranteeing straightforward additivity of these localized orbitals and their properties.

In Natural Population Analysis[66] a molecular wave function is partitioned into a set of maximally occupied NAOs by block-diagonalization of Γ. Natural charges are the total populations of these atom-centered, localized NAOs and exhibit greater numerical stability than Mulliken populations. NBOs and the closely related NHOs are also based on Γ, but are derived from one- and two-atom subblocks.[67,68] Bonding NBOs can be partitioned into single-atom contributions in the NAO basis. These are normalized to form single-atom NHOs, so that any bonding NBO θ_i can be expressed as a linear combination of NHOs $h^{(i)}{}_A$, $h^{(i)}{}_B$, as follows:

$$\theta_{AB} = c_A h_A + c_B h_B \tag{1}$$

where

$$c_A{}^2 + c_B{}^2 = 1$$

In eq 1, c_A and c_B are the *polarization coefficients*, whose squares represent the percentage contribution of the corresponding hybrids to the bond. Each NHO can also be expressed as a linear combination of NAOs, $sp^n d^m$, where n and m are the *hybridization coefficients* and are not necessarily integers.

For neutral atoms in closed-shell molecules, bond polarization has been attributed to the difference in so-called electronegativities of the two participating atoms.[4] Natural electronegativities $\chi_A{}^{(N)}$ are based on polarization coefficients from the natural bond orbitals of a molecular wave function, unlike most electronegativity scales, which refer to properties of isolated atoms.[19i] Ionicity is straightforwardly defined as the difference between the squared NBO polarization coefficients c_A and c_H for an A–H bond:

$$i_{AH} \equiv c_A{}^2 - c_H{}^2 \tag{2}$$

For any atom A, $\chi_A{}^{(N)}$ is then defined on the basis of the average ionicity i_{AH} of bonds in the neutral, valency-saturated compound AH_n:[19i]

$$\chi_A{}^{(N)} \equiv \chi_H{}^{(N)} - \frac{\ln(1 - i_{AH})}{0.45} \tag{3}$$

where

$$\chi_H{}^{(N)} \equiv 2.10$$

For main-group elements used in this study, the resulting values are not far from the traditional Pauling electronegativity scale: $\chi_C{}^{(N)}$

Table 1. Average Computed Transition Metal–Hydrogen Bond Dissociation Enthalpies (av D_e) and Standard Deviations (SD)[a] as Compared with Experimentally Determined Intrinsic Bond Enthalpies by Row, Reported in kcal/mol

this work	row 1		row 2		row 3	
	av D_e	SD	av D_e	SD	av D_e	SD
neutral	53	9	65	7	73	7
cationic	48	6	67	10	75	7

intrinsic	row 1		row 2	
	$E_p = 0$	ref	$E_p = 0$	ref
neutral	58	20		
cationic	56	20	62	23

[a] SD is defined as $s = \sqrt{\dfrac{1}{N-1}\displaystyle\sum_{i=1}^{N}(x_i - \bar{x})^2}$.

$= 2.60$; $\chi_N{}^{(N)} = 3.07$; $\chi_O{}^{(N)} = 3.48$; $\chi_F{}^{(N)} = 3.89$; $\chi_P{}^{(N)} = 2.06$; $\chi_B{}^{(N)} = 1.86$. For transition metals in groups 3–11 except La,[69] natural electronegativity values vary between $\chi_Y{}^{(N)} = 1.09$ and $\chi_{Pt}{}^{(N)} = 2.30$, as summarized in Table 6. Early transition metals usually are less electronegative than the late metals; however some late metals exhibit low electronegativities, notably silver with $\chi_{Ag}{}^{(N)} = 1.48$.

4. Results

Homolytic bond dissociation energies (D_e) were computed for valency-saturated compounds of the form H_nM–X, representing selected ligands (X = H, CH_3, C_2H_5, C_2H_3, C_2H, CH_2F, NH_2, OH, and F) and metals in groups 3–11. Au–H and Pt–H bond dissociation in hypervalent LAu–H and L_2PtH–H complexes (L = Lewis donor) also was studied to illustrate the influence of 3c/4e bonding on metal–ligand bond enthalpies. Although zero-point corrections were not included, differences between calculated D_e and D_0 enthalpies at 0 K are expected to be relatively small. Where applicable, comparisons have been drawn between the present body of computed and measured bond enthalpies extant in the literature. Trends in the metal–ligand bond enthalpies were noted as the metals vary across a row or down a period. The following issues were examined in the light of such comparisons: (1) the idea of "intrinsic" metal–hydrogen and metal–methyl bond enthalpies for all metals in a given row; (2) effect of overall molecular charge on metal–hydrogen and metal–methyl bond enthalpies in isoelectronic compounds; (3) transferability of metal–hydrogen and metal–carbon bond enthalpies among complexes of the same metal; (4) trends in relative metal–ligand bond enthalpies for a series of ligands; (5) correlations between bond polarization and bond enthalpy; and (6) secondary electronic interactions other than σ bonding.

A. Metal–Hydrogen Bond Dissociation Enthalpies. As shown in Figure 2, H_nM–H bond enthalpies vary significantly across a row, contradicting the idea that metal–hydrogen bond enthalpies should remain constant for all metals. H_nM–H bond

(64) Glendening, E. D.; Badenhoop, J. K.; Reed, A. E.; Carpenter, J. E.; Bohmann, J. A.; Morales, C. M.; Weinhold, F. *NBO 5.0*; Theoretical Chemistry Institute, University of Wisconsin: Madison 2001.

(65) Löwdin, P.-O. *Phys. Rev.* **1955**, *97*, 1474.

(66) (a) Reed, A. E.; Weinhold, F. *J. Chem. Phys.* **1983**, *78*, 4066 (b) Reed, A. E.; Weinstock, R. B.; Weinhold, F. *J. Chem. Phys.* **1985**, *83*, 735

(67) Foster, J. P.; Weinhold, F. *J. Am. Chem. Soc.* **1980**, *102*, 7211

(68) Three-center NBOs may also be formed when specifically requested. See the reference below: Weinhold, F. *NBO 5.0 Manual*; Theoretical Chemistry Institute, University of Wisconsin: Madison: Madison, WI, 1996–2001.

(69) NBO analysis was not carried out for La, due to an incompatibility with the basis set.

(70) Parker, V. D., Jr.; Handoo, K. L.; Roness, F.; Tilset, M. *J. Am. Chem. Soc.* **1991**, *113*, 7493–7498.

Table 2. Computed (D_e) and Experimental (D_0 or D_{298}) First M−H Bond Dissociation Energies

computed species	D_e	experimental species	D_0 or D_{298}	method (temperature) and ref
ScH_3	69.0	ScH	48.0[b]	high temp mass spec (0 K)[23]
TiH_4	58.5	TiH	45.2[b]	ion beam mass spec (0 K)[20]
TiH_2^+−H	43.8	Ti^+−H	53.3[b]	ion beam mass spec (0 K)[20]
VH_5	42.8	VH	49[b]	ion beam mass spec (0 K)[20]
VH_3^+−H	47.4	V^+−H	47.3[b]	ion beam mass spec (0 K)[20]
VH_3^+−H	47.4	$(CO)_6V^+$−H	52.6	proton affinity + IP (298 K)[6]
CrH_6	48.0	CrH	44.5[b]	ion beam mass spec (0 K)[20]
CrH_6	48.0	$(CO)_4Cr$−H	54.3	proton affinity + IP (298 K)[23]
CrH_6	48.0	$(Cp)(CO)_3Cr$−H	61.5	proton affinity + IP (298 K)[70]
CrH_4^+−H	36.9	Cr^+−H	31.5[b]	ion beam mass spec (0 K)[20]
CrH_4^+−H	36.9	$(CO)_6Cr^+$−H	54.9	proton affinity + IP (298 K)[23]
MnH_5	55.9	MnH	38.9[b]	ion beam mass spec (0 K)[71]
MnH_5	55.9	$(CO)_5Mn$−H	68.0	proton affinity + IP (298 K)[71]
MnH_3^+−H	45.4	Mn^+−H	47.6[b]	ion beam mass spec (0 K)[20]
MnH_3^+−H	45.4	$(CO)_5Mn^+$−H	41.1	proton affinity + IP (298 K)[23]
FeH_4	43.6	FeH	34.4[b]	ion beam mass spec (0 K)[20]
FeH_4	43.6	$(Cp)(CO)_2Fe$−H	57.1	proton affinity + IP (298 K)[71]
FeH_4^+−H	56.9	Fe^+−H	48.8[b]	ion beam mass spec (0 K)[20]
FeH_4^+−H	56.9	$(CO)_5Fe^+$−H	71.5	proton affinity + IP (298 K)[23]
CoH_3	47.8	CoH	43[b]	ion beam mass spec (0 K)[20]
CoH_3	47.8	$(CO)_4Co$−H	66.4	proton affinity + IP (298 K)[71]
CoH_3^+−H	52.9	Co^+−H	45.7[b]	ion beam mass spec (0 K)[20]
CoH_3^+−H	52.9	$(CO)_2(Cp)Co^+$−H	58.6	proton affinity + IP (298 K)[23]
NiH_2	51.5	NiH	56.2[b]	ion beam mass spec (0 K)[20]
NiH_2^+−H	50.0	Ni^+−H	38.7[b]	ion beam mass spec (0 K)[72]
NiH_2^+−H	50.0	$(CO)_4Ni^+$−H	59.3	proton affinity + IP (298 K)[6]
CuH	61.9	CuH	60.0	ion beam mass spec (0 K)[20]
CuH^+−H	53.2	Cu^+−H	21.0[b]	ion beam mass spec (0 K)[20]
ZrH_4	74.4	$(H)(Cp^*)_2Zr$−H	78	solution calorimetry (298 K)[6]
ZrH_2^+−H	64.1	Zr^+−H	52.1[b]	ion beam mass spec (0 K)[72]
NbH_3^+−H	62.2	Nb^+−H	52.6[b]	ion beam mass spec (0 K)[72]
NbH_3^+−H	62.2	$(CH)Nb^+$−H	64	photodissociation (298 K)[72]
MoH_6	63.3	MoH	46[b]	ion molecule reactions (298 K)[72]
MoH_6	63.3	$(Cp)(CO)_3Mo$−H	69.2	proton affinity + IP (298 K)[71]
MoH_4^+−H	60.7	Mo^+−H	39.7[b]	ion beam mass spec (0 K)[37]
MoH_4^+−H	60.7	$(CO)_6Mo^+$−H	62.1	proton affinity + IP (298 K)[23]
RuH_4	67.7	RuH	52.3[b]	ion beam mass spec (0 K)[72]
RuH_4	67.7	$(Cp)(CO)_2Ru$−H	64.9	proton affinity + IP (298 K)[71]
RuH_4^+−H	74.1	Ru^+−H	37.4[b]	ion beam mass spec (0 K)[72]
RuH_4^+−H	74.1	$(Cp)_2Ru^+$−H	64.8	proton Affinity + IP (298 K)[23]
RhH_3	70.1	RhH	55.8[b]	ion beam mass spec (0 K)[72]
RhH_3	70.1	(octaethylporphyrin)Rh−H	61.9	solution equilibrium (298 K)[6]
RhH_3^+−H	81.3	Rh^+−H	38.5[b]	ion beam mass spec (0 K)[72]
RhH_3^+−H	81.3	$(CO)_2(Cp)Rh^+$−H	68.6	proton affinity + IP (298 K)[6]
PdH_2^+−H	73.1	Pd^+−H	47.7[b]	ion beam mass spec (0 K)[72]
AgH	52.1	AgH	47.5	ion beam mass spec (0 K)[72]
AgH^+−H	49.3	Ag^+−H	9.5[b]	ion beam mass spec (0 K)[72]
HfH_4	81.6	$(H)(Cp^*)_2Hf$−H	80	solution calorimetry (298 K)[6]
HfH_2^+−H	70.2	Hf^+−H	45.4[b]	ion beam mass spec (0 K)[73]
TaH_3^+−H	73.1	Ta^+−H	52.3[b]	ion beam mass spec (0 K)[37]
WH_6	67.8	$(Cp)(CO)_3W$−H	72.3	proton affinity + IP (298 K)[71]
WH_6	67.8	$(I)(Cp)_2W$−H	65.2	solution calorimetry (298 K)[6]
WH_4^+−H	63.1	$(CO)_6W^+$−H	61.4	proton affinity + IP (298 K)[6]
WH_4^+−H	63.1	W^+−H	55.0[b]	ion beam mass spec (0 K)[37]
ReH_5^+−H	70.3	Re^+−H	52.8[b]	ion beam mass spec (0 K)[74]
ReH_5^+−H	70.3	$(CO)_5(CH_3)Re^+$−H	73	proton affinity + IP (298 K)[26]
IrH_3	80.3	$Cl_2(CO)(PPh_3)_2Ir$−H	58.6	solution calorimetry (298 K)[6]
IrH_3^+−H	83.0	Ir^+−H	71.9[b]	ion beam mass spec (0 K)[75]
PtH_2	81.0	PtH	79.3[b]	spectroscopic (0 K)[23]
PtH_2^+−H	84.7	Pt^+−H	64.8[b]	ion beam mass spec (0 K)[37]
AuH	71.0	AuH	68.9	high temp mass spec (0 K)[23]
AuH^+−H	76.6	Au^+−H	50.0[b]	high temp mass spec (0 K)[76]

[a] Experimental bond enthalpies, D_0 or D_{298}, are listed as reported in the literature. See the accompanying references for detailed explanations of the methodology of measurement and any thermal corrections. Experimental bond enthalpies for coordinatively saturated compounds that differ from computed bond energies for the same metal by more than 5 kcal/mol are italicized. [b] Values do not include corrections for exchange and promotion effects.

enthalpies do not vary linearly or even monotonically, and large standard deviations of 7−9 kcal/mol exist across a given row. Similarly large standard deviations and erratic trends exist among "bond strengths" calculated before geometric reorganization of H_nM radicals. No significant correlation exists between the computed bond enthalpies and periodic properties such as the number of hydride ligands, sd^n hybridization at the metal, or average H_nM−H bond polarization. The overall variability

of calculated H_nM−H bond enthalpies undermines the concept of an intrinsic bond enthalpy for each row.

i. Effect of Overall Molecular Charge. Although *average* H_nM^+−H and H_nM−H bond enthalpies are similar within a given row (Table 1), *isoelectronic* H_nM^+−H and H_nM'−H bond enthalpies can differ by as much as 10 to 20 kcal/mol. Figure 3 depicts these differences, illustrating that bond enthalpies in isoelectronic species are not influenced uniformly by charge

Table 3. Properties of Hypervalent LAu−H and L₂PtH−H Complexes: M−H Bond Enthalpies (D_e, kcal/mol); Distances (R(M−H), Å); % Ionicity of the M−H Bond

	ligand				
	(none)	PF₃	PH₃	CO	NH₃
D_e					
LAu−H	71	83	84	90	89
cis-L₂PtH−H	81	85	85	86	90
trans-L₂PtH−H	81	74	76	70	80
R(M−H)					
LAu−H	1.542	1.594	1.594	1.595	1.594
cis-L₂PtH−H	1.520	1.595	1.592	1.596	1.559
trans-L₂PtH−H	1.520	1.648	1.656	1.651	1.670
% ionicity(M−H)[a]					
LAu−H	−4%	−11%	−15%	−18%	−15%
cis-L₂PtH−H	8%	7%	2%	−1%	−4%
trans-L₂PtH−H	8%	1%	−4%	3%	−19%

[a] Negative M−H bond ionicity values indicate polarization toward H.

Table 4. Computed Average Transition Metal−Methyl Bond Dissociation Enthalpies (av D_e) and Standard Deviations (SD)[a] as Compared with Experimentally Determined Intrinsic Bond Enthalpies by Row in kcal/mol

	row 1		row 2		row 3	
this work	av D_e	SD	av D_e	SD	av D_e	SD
neutral	49	8	57	9	67	7
cationic	46	10	63	9	79	4
intrinsic	$E_p = 0$	ref				
neutral	49	22				
cationic	58	20				

[a] SD is defined as $s = \sqrt{\dfrac{1}{N-1}\sum\limits_{i=1}^{N}(x_i-\bar{x})^2}$.

for all metals. For early metals and group 10 metals, metal−hydrogen bonds are predicted to be stronger in neutral compounds than in the isoelectronic cations. The reverse is true for metals in groups 7−9. For first-row metals, neutral metal−hydrogen bond enthalpies are generally stronger relative to those of the isoelectronic cations than for the corresponding second- and third-row metals.

ii. Comparison between Computed and Experimental M−H Bond Enthalpies. Experimentally measured metal−hydrogen bond enthalpies comprise two classes of molecules: coordinatively saturated molecules and highly unsaturated gas-phase molecules or ions of the form MH or MH₂. M−H bond enthalpies in highly unsaturated molecules contain fairly large exchange and promotion contributions, while those of valency-saturated compounds do not. To eliminate ambiguities resulting from exchange and promotion terms, "intrinsic" M−H bond enthalpies[20,23] extrapolated from measurements on highly unsaturated diatomics are compared with those computed for valency-saturated hydrides of all metals within a given row. M−H bond enthalpies for coordinatively saturated species need not be corrected for exchange or promotion energy and are therefore compared directly to those computed for the valency-saturated hydrides of the same metal and overall charge. On the other hand, M−H bond enthalpies in typical coordinatively saturated species are influenced by sterically demanding ligand sets, electronic characteristics of ligands other than H, and energetic consequences of hypervalency. Exceptions to this general classification are the neutral group 11 diatomics CuH, AgH, and AuH, which are valency-saturated and have been observed experimentally.

iii. Average H_nM−H Bond Enthalpies and the Intrinsic Bond Enthalpy. The average of H_nM−H bond enthalpies within a row is at least equally representative of early and late metals,

due to the lack of a monotonic trend. These averages, which are presented in Table 1, provide natural points for comparison with row-dependent trends in experimentally determined intrinsic bond enthalpies.[20,23] Average bond enthalpies in first-row neutral and cationic species are 53 and 48 kcal/mol, respectively, compared with intrinsic bond enthalpies[20] of 58 and 56 kcal/mol. Average bond enthalpies for neutral and cationic species in the second row are considerably stronger than for first-row metals, in agreement with the increased intrinsic M⁺−H bond enthalpy[23] of 62 kcal/mol. In line with predictions based on a few experimental bond enthalpies, average H_nM−H bond enthalpies are even greater for third-row neutral and cationic species.

iv. H_nM−H Bond Enthalpies versus L_nM−H Bond Enthalpies in Coordinatively Saturated Species. For a given metal M, computed H_nM−H and H_nM⁺−H bond enthalpies are in general *not* the same as those measured in solution for coordinatively saturated compounds L_nM−H and L_nM⁺−H. As shown in Table 2, a number of differences greater than 10 kcal/mol arise between computed H_nM−H and H_nM⁺−H bond enthalpies and experimental bond enthalpies for species with the same metal and overall charge. For metals in a given row, root-mean-square differences between computed and experimental values are generally larger than the spread in experimental L_nM−H bond enthalpies. Clearly, "auxiliary" ligands in coordinatively saturated compounds exert a profound influence on metal−hydrogen bond enthalpies. Nevertheless, *average* empirical L_nM−H bond enthalpies for metals within a given row are reasonably similar to the corresponding average for computed H_nM−H bond enthalpies.

v. 3c/4e Bonding and Ligand Effects. One of the key differences between valency-saturated and coordinatively saturated compounds is that 3c/4e bonding must formally occur in the latter. Energetic and structural consequences of 3c/4e bonding are apparent in a few simple, hypervalent Au and Pt compounds. Strikingly, 3c/4e bonding stabilizes linear L−M−M (*trans*) arrangements that are not seen in the equilibrium structures of simple, valency-saturated MH_n compounds. Another consequence of 3c/4e bonding is a change in M−H bond ionicity, as defined in eq 2. Calculated metal−hydrogen bond enthalpies, bond distances, and ionicity parameters are summarized in Table 3 for species of the form LAu−H, *cis*-L₂-PtH−H, and *trans*-L₂PtH−H, with dative ligands L = NH₃, CO, PH₃, and PF₃, having valence electron counts of 14, 16, and 16 around the metal.

The effect of additional dative ligands on M−H bonds in hypervalent species depends on whether they are coordinated *cis* or *trans* to the M−H bond. In *trans*-L₂PtH₂ species, Pt−H bonds opposite a second hydride ligand are significantly lengthened and weakened relative to those in valency-saturated HPt−H, as shown in Table 3. Bond enthalpies vary with dative ligands *cis* to the dissociated Pt−H bond in the order L = NH₃ > PH₃ > PF₃ > CO. For compounds of the form LAuH and *cis*-L₂PtH₂, a dative ligand is coordinated *trans* to each M−H bond. Au−H and Pt−H bonds opposite a dative ligand are slightly longer than in Au−H and HPt−H, respectively. In contrast to the weaker bonding in *trans*-L₂PtH₂ species, Pt−H bonds in *cis*-L₂PtH₂ isomers are stronger than those in PtH₂. Similarly, in compounds of the form LAuH, the Au−H bonds are stronger than that of diatomic AuH. *cis*-L₂PtH−H bond enthalpies increase in the order PF₃ = PH₃ < CO < NH₃, while LAu−H bond enthalpies increase in the order PF₃ < PH₃ < NH₃ < CO.

Table 5. Computed (D_e) and Experimental (D_0 or D_{298}) First M−CH$_3$ Bond Dissociation Energies in kcal/mol[a]

computed species	D_e	experimental species	D_0 or D_{298}	method (temperature) and ref
ScH$_2$CH$_3$	65.4	ScCH$_3$	27.7[b]	ion beam mass spec (0 K)[37]
TiH$_3$CH$_3$	59.2	TiCH$_3$	41.6[b]	ion beam mass spec (0 K)[37]
TiH$_2$$^+$−CH$_3$	55.2	Ti$^+$−CH$_3$	51.1[b]	ion beam mass spec (0 K)[37]
VH$_4$CH$_3$	45.0	VCH$_3$	40.4[b]	ion beam mass spec (0 K)[37]
VH$_3$$^+$−CH$_3$	51.4	V$^+$−CH$_3$	46.1[b]	ion beam mass spec (0 K)[37]
CrH$_5$CH$_3$	43.8	CrCH$_3$	33.5[b]	ion beam mass spec (0 K)[37]
CrH$_4$$^+$−CH$_3$	40.5	Cr$^+$−CH$_3$	31.5[b]	ion beam mass spec (0 K)[37]
MnH$_4$CH$_3$	45.1	MnCH$_3$	20.0[b]	ion beam mass spec (0 K)[37]
MnH$_4$CH$_3$	45.1	(CO)$_5$Mn−CH$_3$	44.7	Calvet microcalorimetry (298 K)[6]
MnH$_5$$^+$−CH$_3$	42.8	Mn$^+$−CH$_3$	49.0[b]	ion beam mass spec (0 K)[37]
FeH$_3$CH$_3$	43.3	FeCH$_3$	32.3[b]	ion beam mass spec (0 K)[37]
FeH$_4$$^+$−CH$_3$	34.0	Fe$^+$−CH$_3$	54.7[b]	ion beam mass spec (0 K)[37]
CoH$_2$CH$_3$	41.0	CoCH$_3$	42.5[b]	ion beam mass spec (0 K)[37]
CoH$_2$CH$_3$	41.0	(dmg)$_2$(py)Co−CH$_3$	33.0	solution calorimetry (298 K)[5]
CoH$_2$CH$_3$	41.0	methylcobalamin	37.0	solution calorimetry (298 K)[77]
CoH$_3$$^+$−CH$_3$	31.7	Co$^+$−CH$_3$	48.5[b]	ion beam mass spec (0 K)[37]
Ni(H)CH$_3$	44.0	NiCH$_3$	49.7[b]	ion beam mass spec (0 K)[37]
NiH$_2$$^+$−CH$_3$	51.2	Ni$^+$−CH$_3$	44.7[b]	ion beam mass spec (0 K)[37]
CuCH$_3$	52.1	CuCH$_3$	53.3	ion beam mass spec (0 K)[37]
CuH$^+$−CH$_3$	59.9	Cu$^+$−CH$_3$	26.5[b]	ion beam mass spec (0 K)[37]
ZrH$_3$CH$_3$	72.3	(Cp*)(CH$_3$)$_2$Zr−CH$_3$	66.0	solution calorimetry (298 K)[6]
ZrH$_2$$^+$−CH$_3$	71.4	Zr$^+$−CH$_3$	55.0[b]	ion beam mass spec (0 K)[37]
NbH$_3$$^+$−CH$_3$	75.9	Nb$^+$−CH$_3$	47.6[b]	ion beam mass spec (0 K)[37]
MoH$_5$CH$_3$	61.6	(Cp)(CO)$_3$Mo−CH$_3$	48.5	solution calorimetry (298 K)[6]
MoH$_4$$^+$−CH$_3$	63.1	Mo$^+$−CH$_3$	37.5[b]	ion beam mass spec (0 K)[37]
RuH$_3$CH$_3$	55.0	RuCH$_3$	38.7[b]	ion beam mass spec (0 K)[73]
RuH$_4$$^+$−CH$_3$	48.8	Ru$^+$−CH$_3$	38.2[b]	ion beam mass spec (0 K)[37]
RhH$_3$$^+$−CH$_3$	60.3	Rh$^+$−CH$_3$	33.9[b]	ion beam mass spec (0 K)[37]
PdH$_2$$^+$−CH$_3$	70.0	Pd$^+$−CH$_3$	43.3[b]	ion beam mass spec (0 K)[37]
AgCH$_3$	39.6	AgCH$_3$	32.0	ion beam mass spec (0 K)[78]
AgH$^+$−CH$_3$	54.8	Ag$^+$−CH$_3$	16.0[b]	ion beam mass spec (0 K) [37]
HfH$_3$CH$_3$	79.6	(Cp*)(CH$_3$)$_2$Hf−CH$_3$	70.3	solution calorimetry (298 K)[6]
HfH$_2$$^+$−CH$_3$	77.9	Hf$^+$−CH$_3$	48.9[b]	ion beam mass spec (0 K)[74]
TaH$_3$$^+$−CH$_3$	87.2	Ta$^+$−CH$_3$	46.8[b]	ion beam mass spec (0 K)[37]
WH$_4$$^+$−CH$_3$	77.9	W$^+$−CH$_3$	53.3[b]	ion beam mass spec (0 K)[79]
ReH$_4$CH$_3$	61.4	(CO)$_5$Re−CH$_3$	52.6	Calvet microcalorimetry (298 K)[6]
ReH$_5$$^+$−CH$_3$	80.0	Re$^+$−CH$_3$	51.2[b]	ion beam mass spec (0 K)[80]
IrH$_3$$^+$−CH$_3$	79.3	Ir$^+$−CH$_3$	74.9[b]	ion beam mass spec (0 K)[81]
Pt(H)CH$_3$	72.2	Cis-(PEt$_3$)$_2$(Cl)Pt−CH$_3$	60.0	Calvet microcalorimetry (298 K)[6]
Pt(H)CH$_3$	72.2	Cis-(PEt$_3$)$_2$(I)Pt−CH$_3$	57.8	Calvet microcalorimetry (298 K)[6]
Pt(H)CH$_3$	72.2	(Cp)(CH$_3$)$_2$Pt−CH$_3$	40.0	gas-phase kinetic studies[6]
PtH$_2$$^+$−CH$_3$	79.3	Pt$^+$−CH$_3$	61.6[b]	ion beam mass spec (0 K)[82]
AuH$^+$−CH$_3$	76.2	Au$^+$−CH$_3$	50.0[b]	ion beam mass spec (0 K)[77]

[a] Experimental bond enthalpies, D_0 or D_{298} are listed as reported in the literature. See the accompanying references for detailed explanations of the methodology of measurement and any thermal corrections. [b] Values do not include corrections for exchange and promotion effects.

As illustrated graphically in Figure 4, ligand effects on M−H bond enthalpies correlate with polarization of the M−H bond toward the hydrogen atom. It is important to note that the *ordering* of ligand effects on M−H bond enthalpies differs with the molecular structure and isomer. In different coordination environments, dative ligands do not always have the same polarizing influence on M−H bonds. For example, the Au−H bond in (CO)Au−H is very polar, while the Pt−H bond in *cis*-(CO)$_2$PtH−H is not very polar. Likewise in *trans*-(NH$_3$)$_2$PtH−H, the Pt−H bond is much more polar than in *cis*-(NH$_3$)$_2$PtH−H. Both *cis*- and *trans*-L$_2$PtH−H bond enthalpies increase as ionicity decreases, but the *trans*-isomer Pt−H bonds are weakened by about 14 kcal/mol relative to those in *cis*-isomers with comparable ionicity.

B. Metal−Methyl Bond Dissociation Enthalpies. Like H$_n$M−H bond enthalpies, H$_n$M−CH$_3$ and H$_n$M$^+$−CH$_3$ bond enthalpies are not constant for metals in a given row (Figure 5). As shown in Table 4, the variability of metal−methyl bond enthalpies within a given row leads to standard deviations (SD) of 7−9 kcal/mol for neutral compounds and 9−10 kcal/mol for cationic complexes of first- and second-row metals. Metal−methyl bond enthalpies computed for third-row cationic species are the least variable, with a 4 kcal/mol SD. The variations do not follow a simple monotonic trend across a given row,

although metal−methyl bonds in neutral species are slightly stronger for early metals than for late metals.

i. Effect of Overall Molecular Charge. Differences between H$_n$M−CH$_3$ and isoelectronic H$_n$M$^+$−CH$_3$ bond enthalpies are highly row-dependent, particularly for early metals. As shown in Figure 6, metal−methyl bonds are stronger in *neutral* complexes of most first-row metals than in the isoelectronic cations. Interestingly, this relationship reverses in passing to second- and third-row metals. Metal−methyl bonds in cationic complexes of third-row metals are, on average, about 10 kcal/mol stronger than in the isoelectronic neutral complexes.

ii. Average H$_n$M−CH$_3$ Bond Enthalpies and the Intrinsic Bond Enthalpy. The average metal−methyl bond enthalpy for first-row metals can be compared to the experimentally determined intrinsic bond enthalpy of 49 kcal/mol. The average computed H$_n$M$^+$−CH$_3$ bond enthalpy for first-row transition metals is 46 kcal/mol with a SD of 10 kcal/mol (Table 4). In contrast, the experimental M$^+$−CH$_3$ intrinsic bond enthalpy for first-row metals is 58 kcal/mol, nearly 10 kcal/mol stronger than for neutral M−CH$_3$ species. Second- and third-row average MH$_n$−CH$_3$ bond enthalpies are somewhat larger than the corresponding first-row values, averaging 57 and 67 kcal/mol. For second- and third-row transition metals, average H$_n$M$^+$−CH$_3$ bond enthalpies are higher than for H$_n$M−CH$_3$ species.

Table 6. Experimental and Calculated $\mathscr{R}^{MC/HC}$ Ratios, $\mathscr{R}^{MX/HX}$ Ratios, and Calculated Natural Electronegativities (χ_N) (residual sums of squares for $\mathscr{R}^{MC/HC}$ fits exceed 0.98)[a]

metal	exptl $R^{MC/HC}$	calc $R^{MC/HC}$	exptl $R^{MX/HX}$	calc $R^{MX/HX}$	calc χ_N
Sc	1.25[44] a	1.8		2.1	1.16
Ti	1.36[43] a	1.5		1.9	1.51
V		1.4		1.6	1.82
Cr		1.3		1.8	2.25
Mn		1.4		0.9	2.15
Fe		1.2		1.3	1.99
Co		1.4		1.3	1.96
Ni		1.4	1.9[29] e	1.0	1.87
Cu		1.5		1.6	1.47
Y		1.9		2.2	1.09
Zr	1[42b] b, ∼0.6[41] c	1.7	∼1[84,41] f	2.0	1.37
Nb		1.5		1.6	1.69
Mo		1.4		1.6	2.10
Tc		1.3		1.3	2.28
Ru	1[27] d	1.3	1[48] g,h	1.1	2.28
Rh	1.22[46] b	1.4		1.0	2.23
Pd		1.3		0.8	1.89
Ag		1.4		1.7	1.48
La		1.8		2.1	i
Hf		1.7		2.0	1.28
Ta	1[42] a,b	1.6		1.7	1.57
W		1.5		1.6	1.93
Re		1.4	1[49], 1.07[85] g	1.4	2.16
Os		1.4		1.0	2.04
Ir	2[45] b	1.5		0.8	2.22
Pt	1[27] d	1.3	1[27] g,h	0.5	2.30
Au		1.2		1.0	2.01

[a] Empirical data include the following substituents: (a) sp^3-, sp^2-, sp-hybridized hydrocarbyls; (b) sp^3-, sp^2-hybridized hydrocarbyls; (c) limited sp^3, sp^2-hybridized hydrocarbyls; (d) limited sp^3-, sp-hybridized hydrocarbyls; (e) N as the sole heteroatom; (f) O as the sole heteroatom; (g) O, N heteroatoms; (h) O, N heteroatoms and limited sp^3- and sp-hybridized hydrocarbyls; (i) NBO analysis is not available for La.[69]

iii. $H_nM−CH_3$ versus $L_nM−CH_3$ Bond Enthalpies in Coordinatively Saturated Species. Empirical metal−methyl bond enthalpies vary significantly from metal to metal and do not match computed $H_nM−CH_3$ bond enthalpies. As shown in Table 5, measured metal−methyl bond enthalpies for coordinatively saturated species are generally weaker than computed $H_nM−CH_3$ bond enthalpies, but M−CH_3 bond enthalpies can be even stronger due to exchange and promotion contributions.

C. Relative Metal−Hydrocarbyl Bond Dissociation Energies.

i. Trends in Relative Metal−Hydrocarbyl Bond Enthalpies. Metal−hydrocarbyl bond enthalpies in representative compounds of the form $H_nM−R$, with R = CH_2CH_3, CH_2F, $CH(CH_3)_2$, $C(CH_3)_3$, $CH=CH_2$, and $C≡CH$, can be directly compared to metal−methyl bond enthalpies for the same metal. Metal-dependent variations in metal−carbon bond enthalpies are fairly consistent. For this reason, effects of substitution and multiple bonding at the α-carbon are best illustrated when $H_nM−R$ bond enthalpies are considered relative to the corresponding metal−methyl bond enthalpies. As shown in Figure 7, metal−carbon bond enthalpies are strongly dependent on properties of the hydrocarbyl substituents.

With increasing substitution at the α-carbon, metal−alkyl bond enthalpies generally decrease. For the hydrocarbyl substituents, calculated bond enthalpies follow the expected ordering for nearly all metals, decreasing as R = CH_3 > CH_2CH_3 > $CH(CH_3)_2$ > $C(CH_3)_3$. For R = CH_2F, the trend is less uniform: metal−carbon bond enthalpies are stronger than those found for R = CH_2CH_3 for metals in groups 4−7, but weaker for other metals. The range of variation is between 10 and 20 kcal/mol, larger for some of the early metals and

smaller for mid to late metals. For comparison, the corresponding range in experimental C−H bond enthalpies is less than 10 kcal/mol.

Unsaturation at the α-carbon substantially increases metal−hydrocarbyl bond enthalpies. Although an increase in metal−carbon bond enthalpy is expected due to greater s-character in the σ-bonding hybrid on carbon, the magnitude of this effect is greater than on C−H bond enthalpies. Calculated metal−vinyl bond enthalpies are stronger than the corresponding metal−methyl bond enthalpies by 2−13 kcal/mol. Calculated metal−ethynyl bond enthalpies are stronger than the corresponding metal−methyl bond enthalpies by nearly 60 kcal/mol for group 3 metals and by at least 35 kcal/mol for late metals. For comparison, the experimental C−H bond enthalpy for HC≡C−H is less than 30 kcal/mol greater than for CH_4. Another noticeable feature is a decline in relative $H_nM−C≡CH$ bond enthalpies from left to right across the d-block.

ii. Comparison between $H_nM−R$ and Hydrocarbon R−H Bond Enthalpies. The relationship between relative $H_nM−R$ bond enthalpies and the corresponding hydrocarbon R−H bond enthalpies is of interest. Calculated metal−hydrocarbyl (M−C) bond enthalpies cover a range of nearly 80 kcal/mol, noticeably larger than the corresponding range of less than 40 kcal/mol in C−H bond enthalpies. This correlation is illustrated in Figure 8 for a particular metal, Ti, by plotting $H_3Ti−R$ bond enthalpies against R−H bond enthalpies. The slope of the best-fit line provides a key ratio, denoted herein by the symbol $\mathscr{R}^{MC/HC}$. A hypothetical 1:1 correspondence would result in a $\mathscr{R}^{MC/HC}$ value of 1. For M = Ti, calculated $H_nM−R$ bond enthalpies lead to a ratio $\mathscr{R}^{MC/HC} = 1.55$. Experimentally, a ratio $\mathscr{R}^{MC/HC} = 1.36$ was found for bulky Ti compounds in a study by Wolczanski and co-workers.[43] Omission of the sp-hybridized (Ti−C_2H) value leads to $\mathscr{R}^{MC/HC} = 1.29$, in excellent agreement with the Wolczanski data.

Table 6 and Figure 9 display the variations in $\mathscr{R}^{MC/HC}$ ratios for all metals as obtained from calculated metal−hydrocarbon bond enthalpies. $\mathscr{R}^{MC/HC}$ ratios are predicted to vary between 1.2 and 1.9 for different transition metals, consistent with the wide range of experimental $\mathscr{R}^{MC/HC}$ ratios. Calculated $\mathscr{R}^{MC/HC}$ ratios are largest among the group 3 metals, decreasing across the early metals. For late metals, $\mathscr{R}^{MC/HC}$ ratios generally fall between 1.2 and 1.5. Calculated $\mathscr{R}^{MC/HC}$ ratios generally do not match those obtained experimentally. This is probably due to the choice of ligands, as others have found good agreement between theoretical and experimental $\mathscr{R}^{MC/HC}$ ratios.[18] The most interesting feature is that larger $\mathscr{R}^{MC/HC}$ ratios are predicted for early metals, consistent with Siegbahn's earlier ab initio study.[13]

D. Relative Metal−Boryl Bond Enthalpies. Metal−boryl bond enthalpies in compounds of the form $H_nM−BH_2$, relative to the corresponding metal−carbon bond enthalpies, are displayed in Figure 10. For early transition metals, these metal−boryl bonds are weaker than the corresponding $H_nM−CH_3$ bonds by 10−15 kcal/mol. In contrast, metal−boryl bonding is stronger than the corresponding $H_nM−CH_3$ bonds by up to 30 kcal/mol for late transition metals. Interestingly, $H_nM−BH_2$ bonds are only about 10−15 kcal/mol stronger than corresponding $H_nM−CH_3$ bonds for late metals in the first row.

E. Nitrogen, Oxygen, and Fluorine Substituents. $H_nM−X$ (X = NH_2, OH, and F) bond enthalpies, relative to those found for $H_nM−CH_3$, are illustrated in Figure 11. For a given substituent X, $H_nM−X$ bond enthalpies decline steadily from left to right across a row. The general ordering of $H_nM−X$ bond enthalpies, X = NH_2 < OH < F, is consistent with the order of ligand electronegativities, as well as with the number of lone
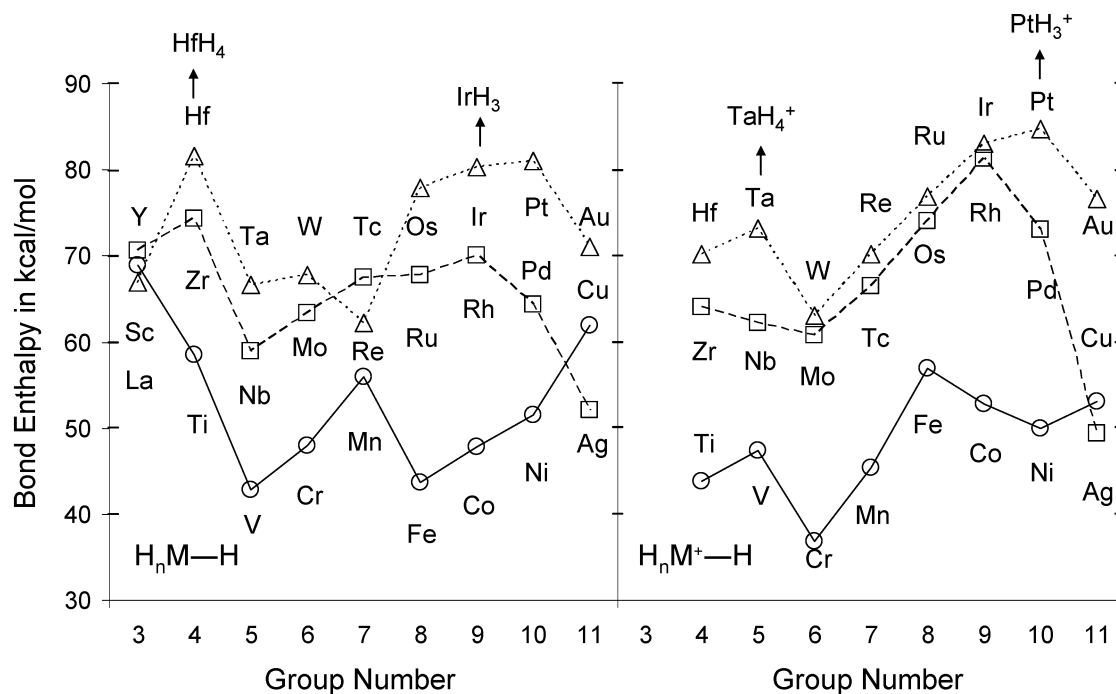
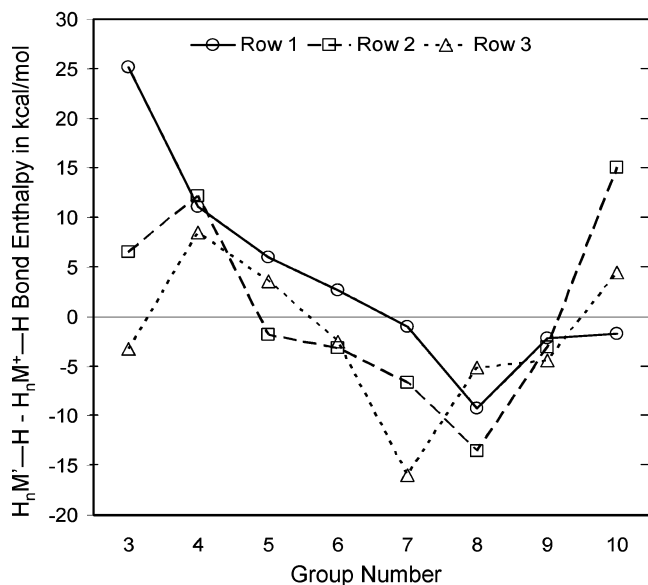**Figure 2.** H_nM-H and H_nM^+-H bond enthalpies (kcal/mol) calculated at the B3LYP level of theory with the triple-ζ LACV3P++** basis set, for valency-saturated neutral and cationic hydride compounds of first-, second-, and third-row transition metals M, as indicated. Circles indicate first-row metals, squares indicate second-row metals, and triangles indicate third-row metals. A cationic valency-saturated hydride compound of a metal in groups 4−11 is isoelectronic to the neutral valency-saturated hydride compound of the metal to its left in a given row. For example, TaH_4^+ and HfH_4 are isoelectronic.

Figure 3. Difference between $H_nM'-H$ and isoelectronic H_nM^+-H bond enthalpies (kcal/mol) calculated at the B3LYP level of theory with the triple-ζ LACV3P++** basis set, for valency-saturated neutral and cationic hydride compounds of first-, second-, and third-row transition metals M', as indicated. Circles indicate first-row metals, squares indicate second-row metals, and triangles indicate third-row metals. Group number on abscissa refers to the neutral metal species M'. See Figure 2 and the accompanying caption for an explanation of isoelectronic species.

pairs on the ligand that could serve as potential π-donors. Among the early transition metals, there is a clear separation between H_nM-X bond enthalpies for X = NH_2, OH, and F. Among the late metals, bond enthalpies vary less with the heteroatom substituent, and in a few cases (Pt, Ag, and Cu) the expected ordering is reversed.

i. Correlation between H_nM-X and $H-X$ Bond Enthalpies. Because metal−heteroatom bond enthalpies vary in the same order as the corresponding H−X bond enthalpies, H_nM-X bond enthalpies for a given metal can be compared with H−X bond enthalpies for the three substituents X = NH_2, OH, and F. Although difficult to interpret in detail with only three substituents, the slope of the best linear fit varies widely between 0.5 and 2.2 for different metals. Poorer correlations are found when both metal−hydrocarbyl and metal−heteroatom bond enthalpies are taken together. $\mathscr{R}^{MX/HX}$ ratios are reported in Table 6 for each metal and are generally not the same as the $\mathscr{R}^{MC/HC}$ ratios. $\mathscr{R}^{MX/HX}$ ratios decrease across the d-block for second- and third-row metals, but the trend is irregular for first-row metals. Somewhat larger $\mathscr{R}^{MX/HX}$ ratios are predicted for early metals, particularly those in groups 3 and 4.

ii. Polarity in Early Transition Metal−Heteroatom Binding. The clear difference between early and late transition metals is illustrated in Figure 12. H_nM-X bond enthalpies relative to H_nM-CH_3 are plotted against the electronegativity difference $(\chi_X^{(N)} - \chi_M^{(N)})$ across the bond. For the early transition metals in groups 3−6, the trend in relative bond enthalpies is consistent: more electropositive metals make more polar and stronger bonds to the heteroatom substituent. For late metals, Figure 12 shows that relative H_nM-X bond enthalpies are *lower* for late metals than would be predicted from the linear fit of early metal−ligand bond enthalpies to electronegativity differences. It is worthwhile noting that valency-saturated late transition metal hydrides have no low-lying orbitals available to accept π-type charge donation from ligand lone pairs.

5. Discussion

A. Are H_nM-H and H_nM-CH_3 Bond Enthalpies "Intrinsic" or "Transferable"? It is clear from the density functional results that H_nM-H and H_nM-CH_3 bond enthalpies vary significantly across a row. Variations from one metal to
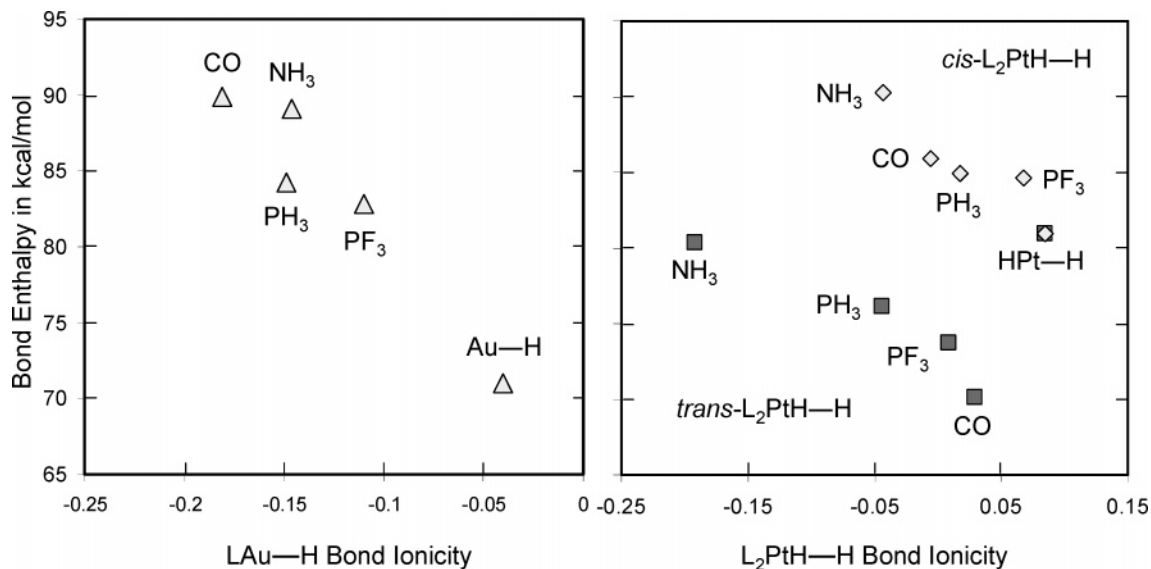
Figure 4. Calculated LAu−H and L₂PtH−H bond enthalpies (kcal/mol) vs M−H bond ionicity for a series of dative ligands L = CO, NH₃, PH₃, PF₃, and none. Triangles indicate LAu−H species, diamonds indicate *cis*-L₂PtH−H species, and squares indicate *trans*-L₂-PtH−H species. Electron count at the metal is >12 for species with dative ligands (14 for LAu−H and 16 for L₂PtH−H).
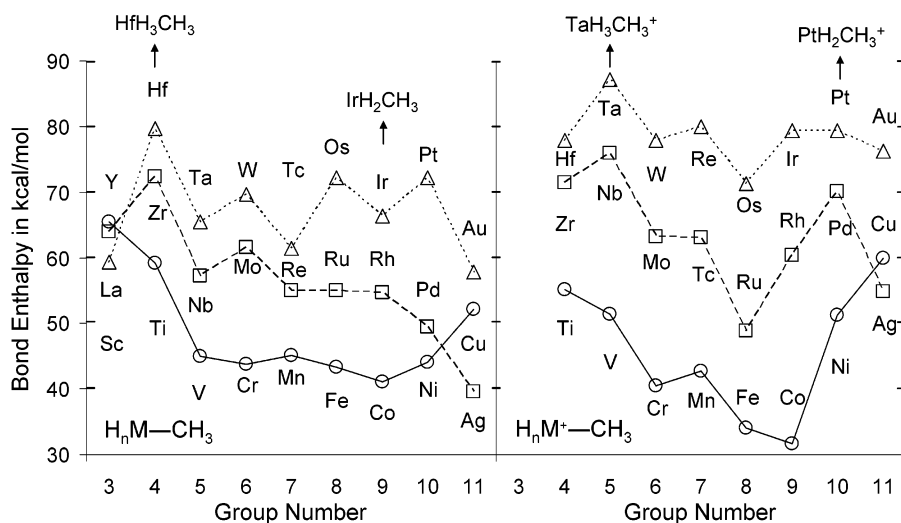

Figure 5. H$_n$M−CH₃ and H$_n$M$^+$−CH₃ bond enthalpies (kcal/mol) calculated at the B3LYP level of theory with the triple-ζ LACV3P++** basis set, for valency-saturated neutral and cationic hydrido-methyl compounds of first-, second-, and third-row transition metals M, as indicated. Circles indicate first-row metals, squares indicate second-row metals, and triangles indicate third-row metals. A cationic valency-saturated compound of a metal in groups 4−11 is isoelectronic to the corresponding neutral valency-saturated compound of the metal to its left in a given row. For example, TaH₃CH₃$^+$ and HfH₃CH₃ are isoelectronic.

the next do not follow a consistent or simple pattern. Average metal−hydrogen and metal−carbon bond enthalpies in a given row are similar in magnitude to available "intrinsic" bond enthalpies that have been extrapolated from experimentally determined M−H and M−CH₃ bond enthalpies. For example, the average H$_n$M−H bond enthalpy for first-row metals is 53 kcal/mol, similar to the intrinsic bond enthalpy of 58 kcal/mol. Still, the clear correlation between bond enthalpies and E_p for highly unsaturated M−H and M−CH₃ compounds in a given row does not extend to valency-saturated compounds (for which $E_p = 0$), because the individual bond enthalpies deviate significantly from the averages.

H$_n$M−H and H$_n$M−CH₃ bond enthalpies also are not generally equal to experimental bond enthalpies of metal−hydrogen or metal methyl bonds in coordinatively saturated compounds of the same metal. On average, computed H$_n$M−H bond enthalpies are similar in magnitude to experimental L$_n$M−H bond enthalpies, but H$_n$M−CH₃ bond enthalpies are somewhat

stronger than L$_n$M−CH₃ bond enthalpies found in the literature. For example, as shown in Table 5, the bond enthalpy D_{298} for Hf(Cp*)(CH₃)₂−CH₃ has been measured at 70.3 kcal/mol, whereas the calculated bond energy D_e for HfH₃−CH₃ is 79.6 kcal/mol. Several others[6,34] have suggested that metal−methyl bonds may be weakened by unfavorable interactions with sterically demanding ligand sets; in any case, metal−methyl bond enthalpies in valency-saturated compounds appear to be different than those in coordinatively saturated organometallics.

B. Substituent Dependence of Metal−Carbon and Metal−Heteroatom Bond Enthalpies. Metal−carbon bond enthalpies are strongly influenced by the degree of substitution and multiple bonding at the α-carbon. The general ordering follows that of the corresponding R−H bond enthalpies: H−C≡CH ≫ H−CH=CH₂ > H−CH₃ > H−CH₂CH₃ > H−CH(CH₃)₂ > H−C(CH₃)₃. When relative H$_n$M−R bond enthalpies are compared to H−R bond enthalpies, an important ratio is the slope of the best linear fit, referred to herein as $\mathscr{R}^{MC/HC}$. This
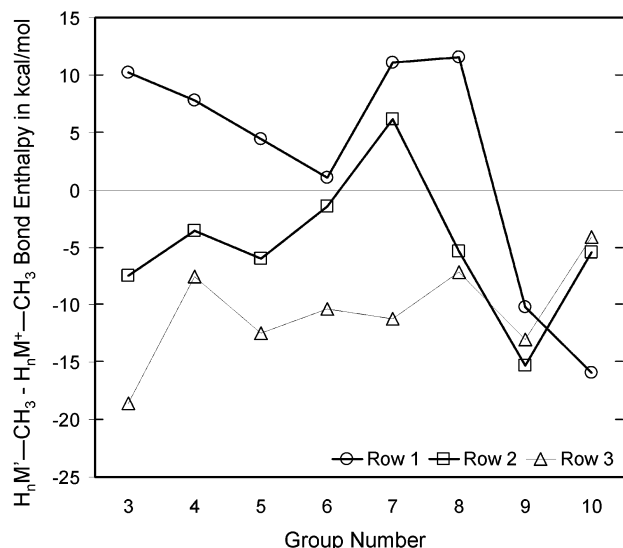
Figure 6. Difference between $H_nM'-CH_3$ and isoelectronic $H_nM^+-CH_3$ bond enthalpies (kcal/mol) calculated at the B3LYP level of theory with the triple-ζ LACV3P++** basis set, for valency-saturated neutral and cationic hydrido-methyl compounds of first-, second-, and third-row transition metals M, as indicated. Circles indicate first-row metals, squares indicate second-row metals, and triangles indicate third-row metals. Group number on abscissa refers to the neutral metal species M'. See Figure 5 and the accompanying caption for an explanation of isoelectronic species.
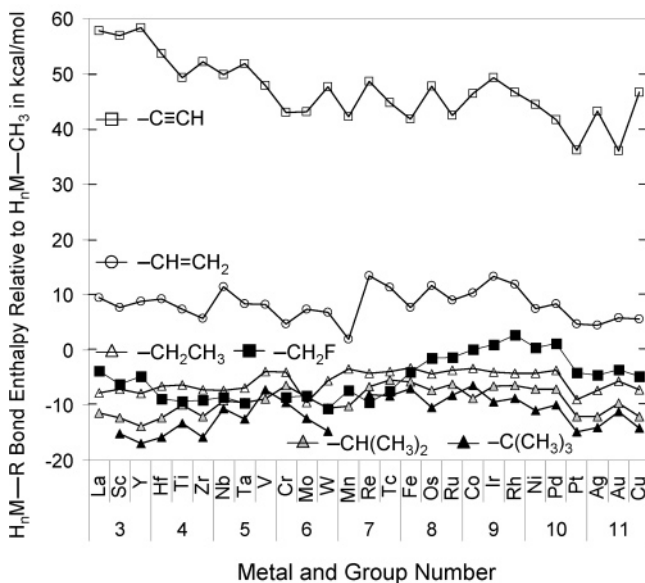
Figure 7. Calculated H_nM-R bond enthalpies (kcal/mol) relative to the H_nM-CH_3 bond enthalpy for the neutral, valency-saturated, hydrido-methyl compound of the same metal M, as indicated by the group number and symbol for M on the abcissa. Different symbols represent hydrocarbyl substituents $-R$, as follows: Open triangles indicate R = CH_2CH_3, open circles indicate R = $CH=CH_2$, open squares indicate R = $C\equiv CH$, shaded triangles indicate R = $CH(CH_3)_2$, and solid triangles indicate R = $C(CH_3)_3$.

ratio varies with the identity of the metal, as shown, along with available experimental values, in Table 6.

Calculated $\mathscr{R}^{MC/HC}$ ratios are somewhat larger for early metals than for late metals. For early metals the $\mathscr{R}^{MC/HC}$ ratios decrease monotonically across a row from groups 3−6. One possible explanation is that increased H_nM-R bond polarity can enhance the differentiation of H_nM-R bond enthalpies for early metals
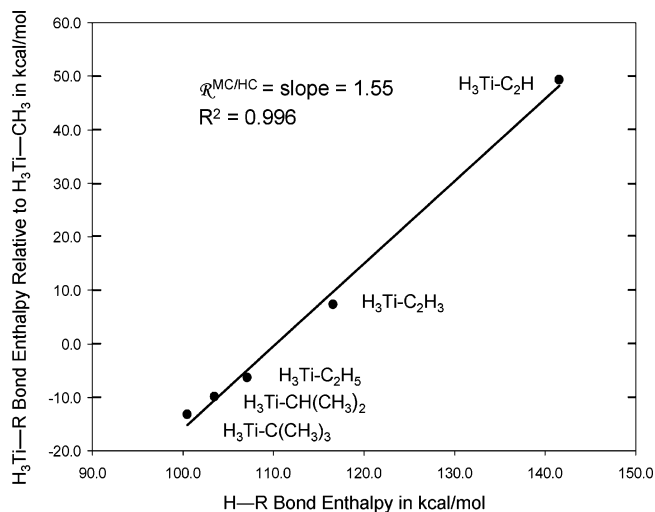

Figure 8. Calculated H_3Ti-R bond enthalpies (kcal/mol) relative to the corresponding H_3Ti-CH_3 bond enthalpy, vs the calculated $H-R$ bond enthalpy for each hydrocarbyl substituent R. Solid trend line is fit to all hydrocarbyl substituents R = C_2H_5, C_2H_3, C_2H, $CH(CH_3)_2$, and $C(CH_3)_3$. The slope of this correlation is referred to as the ratio $\mathscr{R}^{MC/HC} = 1.55$. Calculated hydrocarbon C−H bond enthalpies reasonably match those given in ref 83.
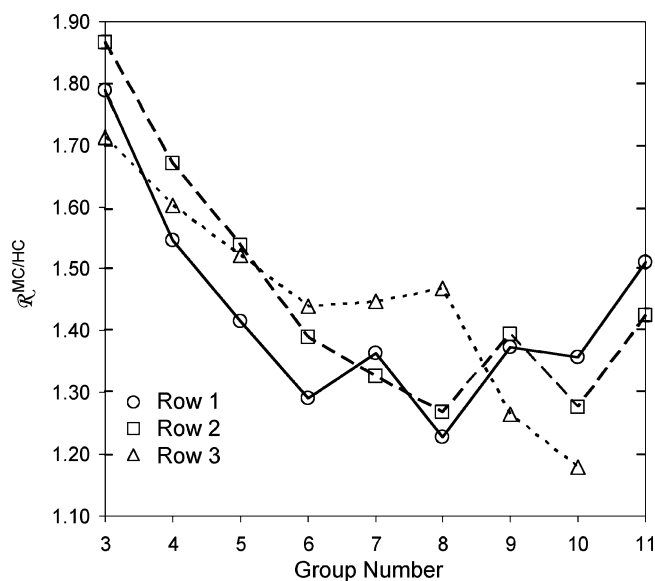

Figure 9. Ratios $\mathscr{R}^{MC/HC}$ from linear fit to H_nM-R vs $H-R$ bond enthalpies for individual metals in rows 1−3, indicated by group number on the abscissa. Circles indicate row 1 metals, squares indicate row 2 metals, and triangles indicate row 3 metals. See Figure 8 for explanation of $\mathscr{R}^{MC/HC}$ ratios.

M. H_nM-R bond polarity was found to decrease from groups 3−6, following the same trend as calculated natural electronegativity values $\chi_M^{(N)}$. For the late metals, calculated $\mathscr{R}^{MC/HC}$ values range from 1.2 to 1.5 and do not follow a simple pattern across a row or correlate with natural electronegativity values.

Similar to the metal−hydrocarbyl bond enthalpies, metal−heteroatom bond enthalpies for a given metal vary in the same order as H−X bond enthalpies for the three substituents X = NH_2, OH, and F. If substituent effects depend solely on radical stabilization, both $\mathscr{R}^{MX/HX}$ and $\mathscr{R}^{MC/HC}$ ratios resulting from a linear best fit correlation should tend toward unity ($\mathscr{R}^{MX/HX} = \mathscr{R}^{MC/HC} = 1$). In the present study, $\mathscr{R}^{MX/HX}$ ratios are generally predicted to differ from $\mathscr{R}^{MC/HC}$ ratios for the same metal.
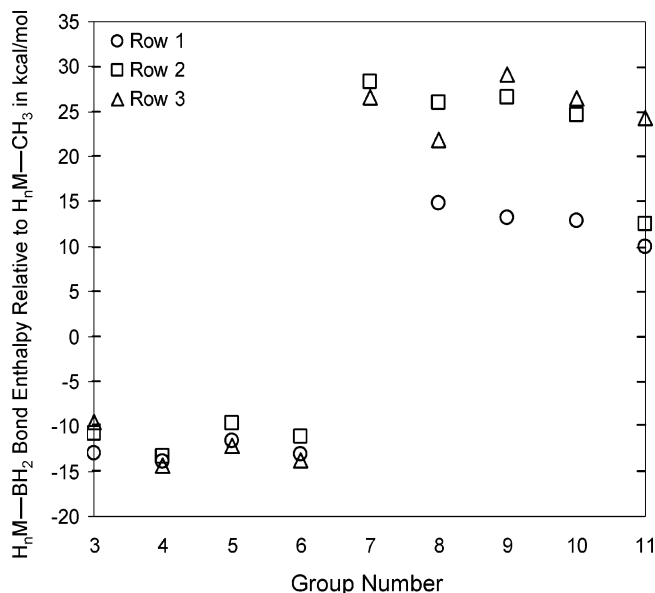
Figure 10. Calculated $H_nM−BH_2$ bond enthalpies (kcal/mol) relative to the $H_nM−CH_3$ bond enthalpy for the neutral, valency-saturated, hydrido-methyl compound of the same metal M, as indicated by the group number and symbol for M on the abcissa.
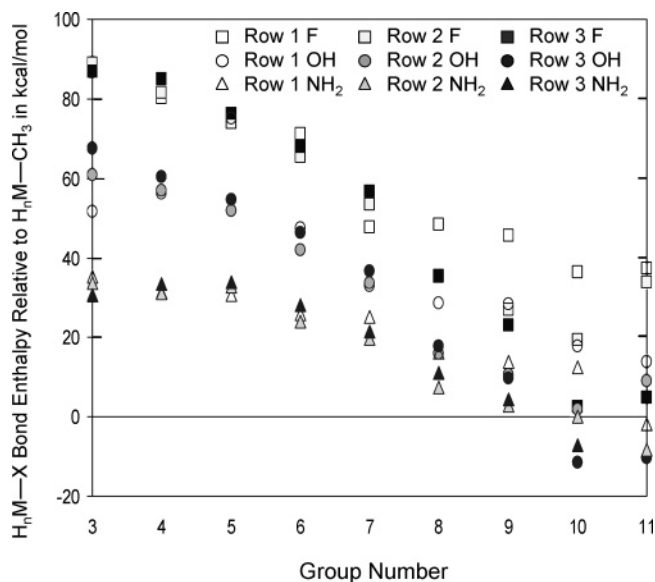

Figure 11. Calculated $H_nM−X$ bond enthalpies (kcal/mol) relative to the $H_nM−CH_3$ bond enthalpy for the neutral, valency-saturated, hydrido-methyl compound of the same metal M, as indicated by the group number and symbol for M on the abcissa. Different symbols represent heteroatomic substituents X, as follows: Triangles indicate R = NH_2, circles indicate R = OH, and squares indicate R = F.

However, both $\mathscr{R}^{MX/HX}$ and $\mathscr{R}^{MC/HC}$ ratios are calculated to be larger for valency-saturated compounds of early metals than of late metals.

C. Effects of Polarity and Lone Pair Interactions on Metal−Heteroatom Bond Enthalpies.

i. π-Bonding between Metal Lone Pairs and Boryl Substituents. The simple, Lewis-like picture above illustrates the advantage of late metal−boryl bonding over the corresponding early metal−boryl bonding. Group 3−6 valency-saturated $H_nM−BH_2$ species have electron counts ≤ 12 and, thus, have no metal lone pairs available for π-bonding. For late metals, particularly the more polarizable metals in rows 2 and 3, valency-saturated $H_nM−BH_2$ compounds have lone pairs avail-

able on the metal center that can donate into the empty p orbital on boron. However, the preference for charge donation from the metal to the BH_2 ligand could also result in bridged bonding between a ligand B−H bond and the metal center. The π-bonding interaction between a metal lone pair and empty p orbital on boron can be associated with substantially stronger $H_nM−BH_2$ bonds for late metals than for early metals, clearly

seen in Figure 10. We note that such π-back-bonding may not be effective when the boron is bound to groups, such as −OR or −NR_2, that are competitive π-donor ligands.[86]

ii. Polarity and Relative Transition Metal−Heteroatom Bond Enthalpies. Relative $H_nM−X$ bond enthalpies decrease across the d-block, but a comparison to natural electronegativity values shows a difference between early and late metals. For the electropositive early metals, increased polarity correlates dramatically with the trend in $H_nM−X$ bond enthalpies. For valency-saturated compounds of early metals, π-type charge transfer from ligand lone pairs to empty metal orbitals is possible, and the degree of charge transfer would be expected to vary strongly with electronegativity differences. Such π-interactions were shown by Armentrout and co-workers[20] to account for a sizable contribution to trends in $M^+−H$ bond enthalpies.

$H_nM−X$ bond enthalpies continue to decline across a row through the late metals, while natural electronegativities do not. The mere absence of empty π-acceptor orbitals on the metal is not sufficient to explain the steady decline of $H_nM−X$ bond enthalpies across a row. In a density functional study by Ziegler and co-workers[87] on coordinatively saturated compounds, a similar trend was attributed to metal−ligand repulsions due to lone pairs on the metal. The horizontal weakening of metal−ligand bonds coincides with the increasing number of lone pairs on valency-saturated late transition metals. This suggests that

(71) Freiser, B. S. In *Organometallic Ion Chemistry*; Freiser, B. S., Ed.; Kluwer Academic Publishers: Dordrecht, 1996.

(72) Armentrout, P. B.; Chen, Y.-M. *J. Am. Soc. Mass Spectrom.* **1999**, *10*, 821−839.

(73) Parke, L. G.; Hinton, C. S.; Armentrout, P. B. *Int. J. Mass Spectrom.* **2006**, in press.

(74) Armentrout, P. B.; Li, F.-X. *J. Chem. Phys.* **2004**, *121*, 248−256.

(75) Li, F.-X. Z., X.-G.; Armentrout, P. B. *J. Phys. Chem. B* **2005**, *109*, 8350−8357.

(76) Li, F.-X.; Armentrout, P. B. *J. Chem. Phys.* **2006**, accepted for publication.

(77) Martin, B. D.; Finke, R. G. *J. Am. Chem. Soc.* **1990**, *112*, 2419−2420.

(78) Chen, Y.-M.; Armentrout, P. B. *J. Phys. Chem.* **1995**, *99*, 11424−11431. Chen, Y.-M.; Elkind, J. L.; Armentrout, P. B. *J. Phys. Chem.* **1995**, *99*, 10438−10445.

(79) Zhang, X.-G.; Armentrout, P. B. *J. Chem. Phys.* **2002**, *116*, 5565−5573.

(80) Armentrout, M. M.; Li, F.-X.; Armentrout, P. B. *J. Phys. Chem. A* **2004**, *108*, 9660−9672.

(81) Li, F.-X.; Zhang, X.-G.; Armentrout, P. B. *Int. J. Mass Spectrom.* **2006**, in press.

(82) Zhang, X.-G.; Liyanage, R.; Armentrout, P. B. *J. Am. Chem. Soc.* **2001**, *123*, 5563−5575.

(83) Blanksby, S. J.; Ellison, G. B. *Acc. Chem. Res.* **2003**, *36*, 255−263.

(84) Diogo, H. P.; Simoni, J. D. A.; Piedade, M. E. M. d.; Dias, A. R.; Martinho Simoes, J. A. *J. Am. Chem. Soc.* **1993**, *115*, 2764−2774.

(85) Reference 29, using data from ref 49.

(86) Cundari, T. R.; Zhao, Y. *Inorg. Chim. Acta* **2003**, *345*, 70−80.

(87) Ziegler, T.; Tschinke, V.; Versluis, L.; Baerends, E. J.; Ravenek, W. *Polyhedron* **1988**, *7*, 1625−1637.
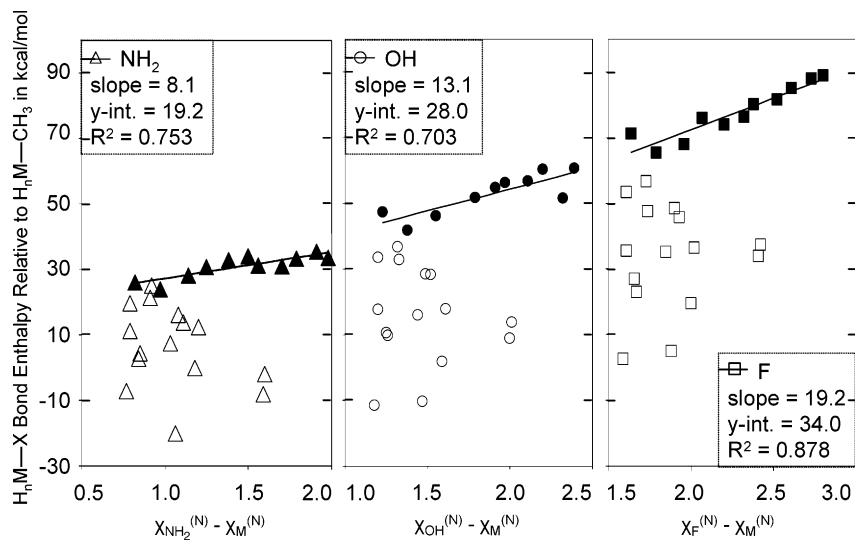
Figure 12. Calculated H_nM-X bond enthalpies (kcal/mol) relative to the H_nM-CH_3 bond enthalpy for the neutral, valency-saturated, hydrido-methyl compound of the same metal M vs difference between natural electronegativities of the heteroatom and the metal ($\chi_X^{(N)} - \chi_M^{(N)}$). Trend lines are fit only to data points corresponding to the early metals in groups 3–6, which are represented by filled symbols. Different symbols represent heteroatomic substituents X, as follows: triangles indicate R = NH_2, circles indicate R = OH, and squares indicate R = F.

trends in calculated late metal–heteroatom bond enthalpies may arise from interactions between ligand and metal lone pairs.

D. Polar Covalent Bonding: A Pauling Relationship? Calculated bond enthalpies and natural electronegativities were fit to a simple empirical correlation. Using Pauling's[4] original geometric-mean formulation (eq 4), the ionic contribution to bond enthalpies is taken as a function of electronegativity differences. The effective natural electronegativity difference was calculated from bond ionicity, according to eq 3, and substituted into the Pauling formula (eq 4). In the resulting formulation (eq 5), electronegativity differences as well as bond enthalpies D_{MA} and D_{AA} can be determined from the ab initio results. D_{MM} values were obtained using eq 5 for A = H while k was chosen to minimize root-mean-square (rms) differences between ab initio bond energies and estimates for D_{MA} obtained from eq 5 for A = CH_3. Another useful approach would be to calculate metal–metal single bond enthalpies D_{MM} at the same level of theory, choosing k to minimize the root-mean-square error in D_{MA} for different ligands A.

$$D_{MA} = \sqrt{D_{MM}D_{AA}} + k|\chi_M - \chi_A| \qquad (4)$$

$$D_{MA} = \sqrt{D_{MM}D_{AA}} + k\left|\frac{\ln(1 - i_{MA})}{0.45}\right| \qquad (5)$$

It was not possible to simultaneously fit the entire body of bond enthalpy data D_{MA} to eq 5. When considering metal–hydrogen and metal–methyl bond enthalpies for all metals, the fitting procedure led to the trivial solution, $k = 0$. When considering only early metals, metal–hydrogen and metal–methyl bond enthalpies could be fit to eq 5 with $k = 8.5$, leading to a satisfactory rms error of 4 kcal/mol in D_{M-CH3}. Using the same constant k, steadily increasing rms errors of 5–15 kcal/mol in D_{MA} were found for early metal–alkyl and early metal–ethenyl bond enthalpies, and values of D_{MM} obtained with early metal–ethynyl and early metal–heteroatom bond enthalpies were unreasonably large. Evidently, eq 5 is not sufficient to describe the trend in bond enthalpies with polarity as ligands are varied substantially. A meaningful comparison to Pauling's formulation would require one or more new terms to express

the strong dependence of bond enthalpies on substituent properties and structural differences between early and late metals.

E. 3c/4e Bonding, *cis*- and *trans*-Ligand Influences in Coordinatively Saturated L_nM-H Bond Enthalpies. *trans*- and *cis*-influences are known examples of the electronic influence exerted by ancillary ligands on thermodynamics in coordinatively saturated transition metal compounds. For example, the destabilization of geometries involving two hydride ligands *trans* to one another in *trans*-L_2PtH_2 compounds is well known. However, the ordering of ligands in a *trans*-influence series is not transferable from one metal to another and must be determined empirically for different metal centers and coordination geometries. The present work suggests that M–H bond polarity influences these trends. *trans*- and *cis*-influences on computed M–H bond enthalpies arise in 14e⁻ LAuH compounds and 16e⁻ L_2PtH_2 compounds with hypervalent 3c/4e bonding (Figure 4). Computed Pt–H bond enthalpies vary between 70 and 90 kcal/mol, depending on the ligand set and geometry. In each series of compounds with different donor ligands, M–H bond enthalpies increase with the polarization of the M–H bond toward H.

6. Conclusions

Homolytic bond enthalpies have been calculated for a comprehensive collection of valency-saturated transition metal hydride species of the form H_nM-X. Using a consistent, minimal ligand set and well-defined electron counts, bond enthalpies for all metals in groups 3–11 were compiled that have minimal influence from the steric interactions, agostic effects, or delocalized 3c/4e bonding interactions that are characteristic of transition metal species with more complex ligand systems.

This work provides a base for the systematic exploration of trends in transition metal–ligand bond enthalpies. Periodic trends in calculated metal–ligand bond enthalpies have been evaluated for several key ligand types. Vertical trends are consistent with those observed experimentally. Within a given row, a substantial difference between the bonding of early and late transition metals is evident.

1. Large Variations in Metal−Ligand Bond Enthalpies across a Row Undermine the Utility of "Intrinsic" Bond Enthalpies. Transition metal−hydrogen and transition metal−methyl bond enthalpies exhibit significant, nonsystematic fluctuations across a row. $H_nM−H$, $H_nM^+−H$, $H_nM−CH_3$, and $H_nM^+−CH_3$ bond enthalpies generally increase down a period, in accord with experimental bond enthalpies. Subtle polarity effects, particularly for charged species, emerge upon detailed analysis. Further calculations are necessary to determine how these metal-dependent variations relate to the wide range of metal−hydrogen and metal−methyl bond enthalpies that are known for coordinatively saturated organometallic complexes.

2. Hybridization and Substitution at the α-Carbon Strongly Influences Transition Metal−Hydrocarbyl Bond Enthalpies. $H_nM−R$ bond enthalpies vary with substituent properties in the same order as $H−R$ bond enthalpies, but not always in a 1:1 ratio. $\mathscr{R}^{MC/HC}$ ratios computed for individual transition metals vary between 1.2 and 1.9, with the larger of these found among the early metals. Increased $\mathscr{R}^{MC/HC}$ ratios for early metals coincide with metal−carbon bond polarization. The strong dependence of metal−carbon bond enthalpies on the nature of the hydrocarbyl substituent is a distinguishing feature that is not adequately described by Pauling's formula (eq 5).

3. Metal−Boryl Bond Enthalpies Clearly Demonstrate π-Bonding. Valency-saturated compounds of late metals have lone pairs that donate into the empty boron p-orbital. Correspondingly, these compounds have consistently higher metal−boryl bond enthalpies, relative to the corresponding metal−methyl bond enthalpies, than valency-saturated compounds of early metals. It is expected that this multiple bonding effect should also be observed in coordinatively saturated metal boryl complexes with filled metal lone pairs.

4. Electron-Pair Bonds to Electronegative Ligands Are Stronger for Early Metals Than Late Metals. Similar to metal−carbon bond enthalpies, metal−heteroatom bond enthalpies exhibit a strong dependence on the heteroatom substituent. Metal−heteroatom bond enthalpies, relative to the corresponding metal−methyl bond enthalpies, decrease from left to right across a given row of the periodic table. Early metal−heteroatom bond enthalpies increase in a trend that is consistent with metal electronegativity, while late metal−heteroatom bond enthalpies do not. Late metal−heteroatom bond enthalpy variations appear to represent a complex interplay between bond polarity and lone pair interactions.

5. Hypervalency Strongly Affects Bond Enthalpies. Coordinatively saturated transition metal complexes are considered to be hypervalent in the context of the 12-electron model. For hypervalent complexes of the form LAu−H and $L_2PtH−H$ over a series of dative ligands L, *trans-* and *cis-*influences on metal−hydrogen bond enthalpies are large. Bond enthalpies increase with the partial charge on H for complexes of the same metal and symmetry. If these results extend to organometallic complexes that are coordinatively saturated, metal−hydrogen bonds opposite dative ligands should be stronger than in valency-saturated species.

This work provides a basic foundation for exploring the factors influencing homolytic metal−ligand bond enthalpies. Further calculations are needed to evaluate the effects of hypervalency on metal−ligand bond enthalpies in typical 18-electron organometallic species. More intensive calibration of the computation methods is needed in order to achieve chemically accurate comparison with experimental bond enthalpies. With these improvements, extension of the present model to more realistic organometallic systems will result in a better understanding of trends in homolytic metal−ligand bond enthalpies.

Supporting Information Available: Computed bond enthalpies, bond lengths, polarization coefficients, partial charges, metal hybridization, and Cartesian coordinates for selected structures. This material is available free of charge via the Internet at http://pubs.acs.org.

OM0603058